UNIVERSITY OF BELGRADE

FACULTY OF TECHNOLOGY AND METALLURGY

Ahmed Ali Salem Awhida

NOVEL METHOD FOR MEASUREMENT OF RADON EXHALATION FROM BUILDING MATERIALS

Doctoral Dissertation

Belgrade, 2017

UNIVERZITET U BEOGRADU TEHNOLOŠKO-METALURŠKI FAKULTET

Ahmed Ali Salem Awhida

NOVI METOD MERENJA EKSHALACIJE RADONA IZ GRAĐJEVINSKIH MATERIJALA

doktorska disertacija

Beograd, 2017.

Table of Contents

CHAPTER

1 Introduction

Radon is a colourless, odourless, tasteless and radioactive gas produced from the natural decay of uranium which is found practically in all types of soils. Radon moves up through the ground and enters into atmosphere of into buildings if they are found on its path. Radon enters into buildings through cracks in the foundation, gaps and joints in the building materials. The other major source of the radon in indoor air is building materials whereas they contain uranium and radium, as well. Thus, radon is considered as a significant contaminant that affects indoor air quality.

The major health risk associated with exposure to radon gas is an increased risk of lung cancer and this is the main reason why the radon is widely investigated all over the world.

1.1 Short history of radioactivity

All begins in the year 1895 with the discovery of Wilhelm Röntgen. In his experiment he covered Hittorf-Crookes tube (an early experimental electrical discharge tube) with a black cardboard. Previously he darkened the room and placed and from a bench a few feet away, he saw a surprising phenomenon: the barium platinocyanide screen placed nearby seemed to be shimmering some green light.

Immediately, Röntgen speculated that a new kind of ray might be responsible for the phenomenon. In this period of investigation, he temporarily used a term "X-rays", as the mathematical designation ("X") for unknown variable or for something unknown, in principle. This temporary term is still used in physics, although in many, especially as a term in medicine, the term "Röntgen Rays" is used and consequently X-ray radiograms are known as "Röntgenograms"). Very soon after this discovery, he took the very first picture using X-rays, using his wife's hand. This became soon the most important tool

in medicine for diagnostic of bone fractures and today, Röntgen is considered as the father of diagnostic radiology.

In 1896 Henri Becquerel was using naturally fluorescent minerals to study the properties of x-rays. He exposed potassium uranyl sulfate to sunlight and then placed it on photographic plates, covered by black cardboard. He expected that this uranium compound could absorb the sun's radiation and then emit it as x-rays. Although it was overcast in Paris, he decided to develop his photographic plates anyway. To his surprise, an image was produces on the photographic plate, and moreover it was strong and clear, which was a proof that the uranium emitted radiation. Effectively, Becquerel was first who discovered radioactivity, as he didn't know what was the nature of this radiation, he named it simply "Uranium radiation".

The term radioactivity itself, was devised by Marie Curie, who together with her husband Pierre, was experimenting on the new phenomenon of "Uranium radiation". The Curies separated uranium from its ore and discovered that the leftovers showed more activity than the extracted uranium. Their conclusion was that the ore also contains other radioactive elements. Only few years later the chemical properties (and their position in the Mendeleyev table) of two elements (Polonium and Radium) were discovered. The name Polonium came from the name of the birth country of Marie Curie – Poland. Consequently Henry Becquerel, Marie Curie and Pierre Curie shared Nobel Prize in Physics in the 1903. She also won the 1911 Nobel Prize in Chemistry.

At the time there was no knowledge of detrimental influence of radioactivity and Marie Curie suffered serious burns on her hands due to direct exposure to alpha rays. She died due to aplastic anaemia which developed due to constant exposure to radioactive sources.

Ernest Rutherford performed many experiments, studying the absorption of radioactivity by thin sheets of metal foils and he found three types of radiation clasifyed by their penetration power and he named them by first letters of Greek alphabet: alpha (α) radiation, absorbed by a few tens of micrometres of metal foil, beta (β) radiation, which can penetrate as much as few millimetres of foil and gamma (γ) rays which can

pass through several centimetres of lead. He also noted that these three kinds are differently affected by electric and magnetic fields.

Ernest Rutherford (with help of Hans Geiger – Gaiger counter inventor) performed one of the most famous experiments in nuclear physics. In his experiment Rutherford used few milligrams of radium as alpha source. The alpha rays were passing through a golden foil in attempt to measure angular scattering of alpha particles recoiled from the golden foil (Figure 1.1). The real experiment was conducted by rotating microscope with the zinc sulphide screen at the end of the microscope. To their great surprise, Rutherford and Geiger discovered that some alpha particles scatter backwards.

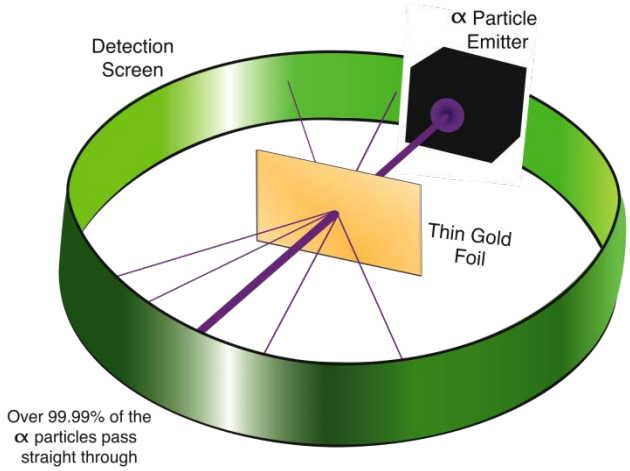

Figure 1.1: Rutherford's experiment.

The only rational explanation was that the most of the matter in the golden foil is concentrated as the positive charge is in a sphere of radius less than 10^{-13} meters and this was the first proof of the existence of atomic nucleus. In 1908 Rutherford was awarded the Nobel Prize for chemistry.

At the end it can be said that the darkest part in the nuclear physics history was the production of atomic bomb, first designed in Los Alamos during the World War II.

1.2 Radiation types

Radiation is the process of emission or transmission of energy in the form of waves or particles through space or through a material medium. In general, radiation is categorized as either ionizing or non-ionizing depending on the energy i.e. on the possibility to ionise the medium where the process occurs. Herein, only the ionizing radiation related to nuclear processes will be considered.

The main process which induces the occurrence of natural radioactivity is the nuclear decay. First condition for a decay to happen is to be energetically plausible. There are three main types of radioactive decay: alpha, beta and gamma decay, but also electronic capture and spontaneous fission. In general if the nucleus has a surplus of protons, the beta plus decay or electronic capture occurs and additionally if the nucleus is also massive, the alpha decay occurs. If the nucleus has a surplus of neutrons, the beta minus decay occurs. Very heavy nuclei undergo spontaneous fission (see Figure 1.2).

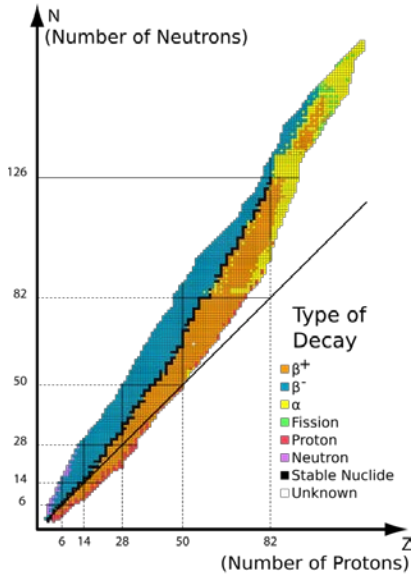

Figure 1.2: Chart of nuclides and corresponding nuclear decays.

1.2.1 Alpha decay

Certain heavy nuclei are energetically unstable against the spontaneous emission of an alpha particle (^{4}He). The probability of decay is governed by the barrier penetration i.e. by quantum mechanical tunnelling. The nucleus is formed of protons and neutrons and at each moment some of them can form one or more alpha particles inside the nucleus. The alpha particle hits the outer Coulomb barrier and in principle recoils back to the bulk of the nucleus, because the energy of the alpha particle is not sufficient to overcome the Coulomb barrier. Due to the quantum mechanical tunneling it is possible that the alpha particle tunnel through the Coulomb barrier, leaving the nucleus, which effectively presents the alpha decay. The decay process is presented by the following formula:

$$ {}^{A}_{Z}X \rightarrow {}^{A-4}_{Z-2}Y + {}^{4}_{2}\alpha $$

where X and Y are the parent and the daughter (or progeny) nuclei.

Typical energies of alpha decay lays between 5 and 7 MeV. When the energy of alpha decay is beyond about 6.5 MeV, the half-life of the nuclei is expected to be less than a few days, while if the energy is lower than 4 MeV, the barrier penetration probability becomes very small and the half-life of the nuclei is very long.

1.2.2 Beta decay and electron capture

Beta decay and electron capture are very similar by their nature – both types are the consequence of the transformation caused by the weak interaction, when one proton in a nucleus is transformed in neutron and vice versa. Additionally, there are two types of beta decay: beta minus and beta plus.

1.2.2.1 Beta minus decay

When a nucleus has too many neutrons it becomes unstable and it will try to stabilize itself and get closer to stability by transforming a neutron into a proton.

To keep charge conservation it must emit an electron and to keep conserved leptonic number, it also emits an electronic anti-neutrino. This process, called beta minus decay, is described as:

$$n \rightarrow p + e^{-} + \bar{\nu_e}$$

The net result for the atom is that the atomic number Z increases by 1 and the atomic mass A does not change. This means that the atom has transformed into the element with the next higher atomic number. The available energy in this decay is transferred both to the electron and to the neutrino. The consequence is that the energy spectrum of emitted beta particle is continuous, unlike the spectrum of alpha particle which is discrete.

1.2.2.2 Beta plus decay

The beta plus decay is very similar to the beta minus since in this case a proton is transformed to a neutron in a nucleus with surplus of protons. In the decay a positron (antimatter counterpart of electron) and electronic neutrino are emitted. The process is described as:

$$p \rightarrow n + e^{+} + \nu_e$$

The emitted positron travels a short distance in the surrounding material before it annihilates with an electron from the surroundings. In the process of annihilation two gamma rays of energy of 511 keV are emitted in opposite directions. The 511 keV gamma ray is a mark of the beta plus decay.

1.2.2.3 Electron capture

The electron capture is practically an inverse beta minus decay, when a proton in the nucleus capture an atomic electron. The process is described as:

$$p + e^{-} \rightarrow n + \nu_e$$

By this process, the number neutrons in a nucleus increases, like in beta plus decay. Actually, the beta plus decay and the electron capture are always in competition.

At lower energies the beta plus decay is less probable since the emitting positron should pass through the Coulomb barrier by the tunneling effect – like in the case of an alpha particle.

1.2.3 Gamma decay and decay of isomers

Gamma decay is different than other decays as it does not transform a nucleus, but transfer it from an excited to ground state. Very often, after beta or alpha decay the nucleus is in excited state and it de-excites by gamma ray emission. In that sense nuclear transitions from an excited state are an integral part of other decay modes. Although these gamma rays belong to de-exciting daughter nucleus, in the table of isotopes these characteristic gamma rays are attributed to the parent nucleus as they emerge directly after the decay of a parent nucleus.

An isomeric transition happens when the excited state is metastable, which means that it has sufficiently long half-life (typically from few seconds up to several hours). In that case, the emission of the gamma ray is not anymore directly related to the decay of the parent nucleus and the decay is considered as a decay of separate nuclide. Well known isomer state is the one of ^{99m}Tc, the most commonly used medical radioisotope, widely used in medical diagnostic procedures. The schematics of the decays of the parent nucleus ^{99}Mo and the isomer ^{99m}Tc (Figure 1.3)

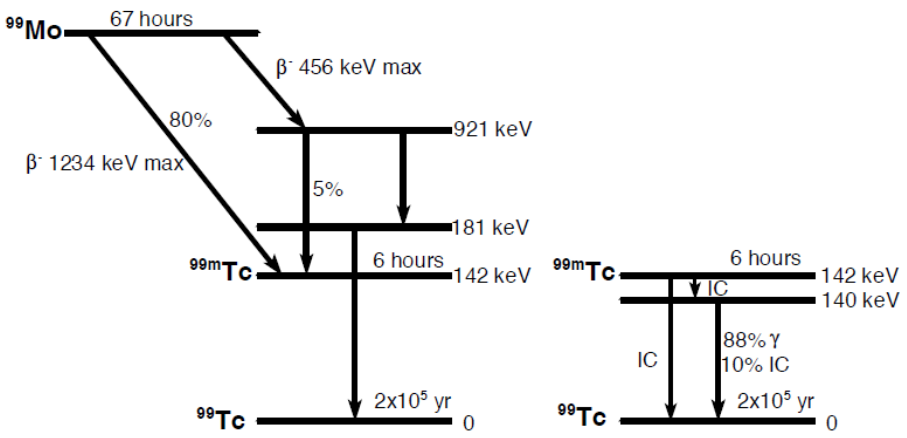

Figure 1.3: Scheme of the decay of ^{99}Mo (left) and the decay of the isomer ^{99m}Tc (right)

^{99}Mo has a half-life of 67 hours and decays by electron emission to 99Tc. About 16% of decay to the state 921 keV and ~5% de-excites to the state 142 keV, emitting a gamma ray of 779 keV, while ~12% decays to the state 181 keV, emitting a gamma ray of 740 keV. The state 181 keV decays to the ground state. Thus, the gamma rays 181 keV, 740 keV and 779 keV are characteristic gamma rays of the decay of ^{99}Mo.

About 85% of ^{99}Mo decays finish at the metastable state at 140 keV which is referred to as ^{99m}Tc. The half-life of this state is ~6 h and it decays to ground state by emitting a gamma ray of 140 keV with the probability of 88%. Evidently, the gamma ray 140 keV is not characteristic gamma ray of the ^{99}Mo decay.

1.3 Radiation interaction with mater

The manner functioning of radiation detectors essentially depends on the way how radiation interacts with the material of the detector itself. Moreover the influence of the radiation on a biological tissue depends on this interaction, as well. It is very important to have a clear knowledge about the response of different types of detectors to a specific type of radiation.

There are four categories of ionising radiation which have fundamentally different interaction with matter: heavy charged particles, fast electrons, neutrons and

X-rays with gamma rays. First two interact mainly by coulomb interaction, while the latter two interact more or less directly.

1.3.1 Interaction with heavy charged particles

Heavy charged particles comprise protons, alphas and other nuclei. These particles interact with matter mainly through Coulomb forces between their positive charge and the negative charge of the orbital electrons of the atoms in the absorbing medium. The interactions with nuclei are possible, however at relevant energies (of environmental radioactivity) such events occur rarely and they are not normally significant in the response of radiation detectors. Thus, charged particle detectors rely on the interactions with electrons in the active (absorbing) media of a detector.

When a charged particle enters an absorbing medium, it interacts with many electrons. The electrons are pushed around by the Coulomb force as the incident charged particle passes by them. Depending on the strength the interaction, the electron pushed by incident particle may raise to a higher-lying shell within the absorber atom (excitation) or to remove completely the electron from the atom (process of ionisation). The process of ionisation produce an ion pair is made up of a free electron and the corresponding positive ion of an absorber atom. The ion pairs have a tendency to recombine, although under certain conditions this recombination is suppressed which is used in some detectors.

The energy that is transferred to the electrons must is coming from the kinetic energy of the incident particle. The process repeats continuously until the incident particles lose all energy. The portion of energy loss in each interaction is very small comparing it with the kinetic energy of the incident particle, thus the energy loss is effectively a continuous process. The path of the incident particle is straight because the particle is not significantly deflected from its original direction by any of the single interaction and interactions occur in all directions simultaneously. Due to this fact

charged particles have very well defined definite range in a given absorber material. The range represents a maximum distance in an absorber which the particle may reach.

1.3.1.1 Stopping power

The stopping power S is a very important parameter in the framework of the interaction of charged particles with matter. It is defined as the differential energy loss along the differential path length:

$$S = -\frac{dE}{dx} \quad \textbf{(1)}$$

The classical expression that describes the energy loss is famous Bethe formula:

$$-\frac{dE}{dx} = \frac{4\pi e^4 z^2}{m_0 v^2} NB \quad \textbf{(2)}$$

Where

$$B = Z\left[\ln\frac{2m_0 v^2}{I} - \ln\left(1-\frac{v^2}{c^2}\right) - \frac{v^2}{c^2}\right] \quad \textbf{(3)}$$

Where v is the velocity of charged particle, ze is the charge, N and Z are the number density and atomic number of the absorber atoms, m_0 is the electron mass, e is the electron charge and c is the velocity of light. The parameter I represents the average excitation and ionisation potential of the absorber. This value has to be determined experimentally. dE/dx varies with $1/v^2$ or with 1/E, which means that the stopping power increases at lower energies. The simple explication of this feature is that the particle stays longer near to an electron which allows it to transfer more of its kinetic energy to a given electron. The stopping power also highly depends on the atomic number.

The Bethe formula seize to be accurate at low energies when the exchange of electrons between the particle and absorber becomes important. At lower energies the positively charged particle will then tend to pick up electrons, reducing its charge which obviously decreases its energy loss, finally becoming neutral atom.

1.3.1.2 Bragg peak

A plot of the energy loss along the path of a charged particle in function of the penetration depth is shown on the Figure 1.4. The maximum stopping power (and the energy transfer) at the end of the charged particle path is called the *Bragg peak*. This feature is important in many areas, such as medical therapies to the solid state nuclear track detectors. Plots on the Figure 4 are showing a single alpha particle track and the average stopping power of a parallel beam of alpha particles of the same initial energy. The difference mainly comes from the effect of straggling.

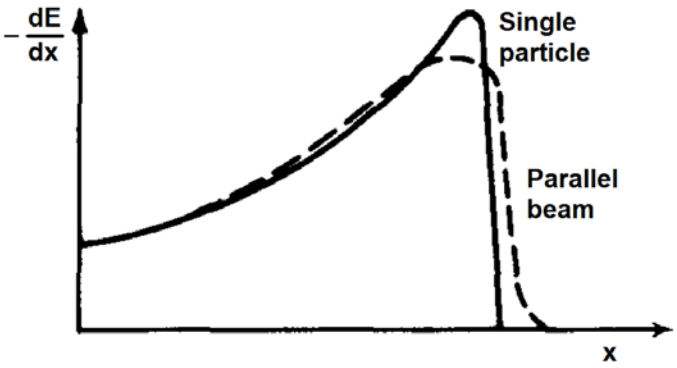

Figure 1.4: The Bragg curve. Stopping power as a function of a penetration depth of a charged particle

1.3.1.3 Energy and range straggling

The energy loss is a stochastic process due to the fact that the overall energy transfer consists of finite number of individual interactions between the incident particle and electrons of the degrader medium. Thus, the monoenergetic beam will always be subject to a spread of the energy. The width of this energy distribution is a measure of *energy straggling*. The straggling depends on the distance along the particle track, but also on the degrader's material.

The *range* of the charged particles of given energy in certain material can be determined in few manners. The mean range is defined as the absorber thickness that reduces the beam intensity (number of incident particles) to one-half of the original intensity. This definition is in general used in range tables. Another important version

of the range definition is the extrapolated range, obtained by extrapolation of the linear part of the end of the transmission curve to zero. Both definitions are graphically explained on the Figure 1.5.

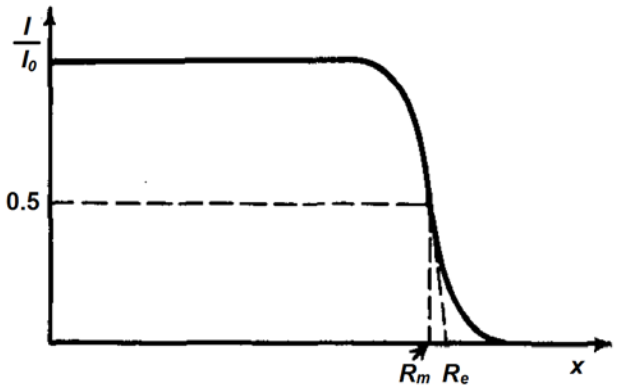

Figure 1.5: The graphical explanation of the mean range R_m and the extrapolated range R_e. I is the intensity of the incident beam after the absorber thickness of x, I_0 is the intensity with no absorber.

The *range straggling* of particles is defined as the fluctuation in path length for individual particles of the same initial energy. In a certain way it is a consequence of the energy straggling as the same stochastic factors that lead to energy straggling are responsible for a difference of total path lengths for each particle of an incident beam. For alpha particles, the straggling is a few percent of the mean range.

1.3.2 Interactions with fast electrons

In comparison with heavy charged particles, electrons of similar energy lose their energy at a lower rate due to the fact that they have a much higher velocity when they have the same energy as heavy particles. Their path is very twisted and the backscattering is not a rare event, while for the heavy charged particles it could be completely neglected. The main reason for such behavior is a lower mass of electron and the fact that they can lose a significant portion of its kinetic energy in a single collision with an orbital electron or significantly change the direction of its movement direction when it collides with a nucleus. A similar expression to similar to that of

equation 3 has also been derived by Bethe for fast electrons which estimates energy loss due to the collisions, mainly with electrons in the absorber:

$$-\left.\frac{dE}{dx}\right|_c = \frac{2\pi e^{'} NZ}{m_0 v^2}\left(\ln\frac{m_0 v^2 E}{2I^2(1-\beta^1)} - (\ln 2)\left(2\sqrt{1-\beta^2}-1+\beta^2\right)+\left(1-\beta^2\right)+\frac{1}{8}\left(1-\sqrt{1-\beta^2}\right)^2\right) \quad \textbf{(4)}$$

However, fast electrons are losing their energy due to the radiation process during the deceleration – so called *bremsstrahlung*:

$$-\left.\frac{dE}{dx}\right|_r = \frac{NEZ(Z+1)e^4}{137 m_0^2 c^4}\left(4\ln\frac{2E}{m_0 c^2}-\frac{4}{3}\right) \quad \textbf{(5)}$$

The total stopping power for fast electrons is the sum of the collisional and radiative losses:

$$\frac{dE}{dx} = \left.\frac{dE}{dx}\right|_c + \left.\frac{dE}{dx}\right|_r \quad \textbf{(6)}$$

The range definition is less explicit for fast electrons than for heavy particles, because the electron total path length is considerably longer than the distance of penetration in the absorber along the initial penetration direction. The stopping power and range of electrons and positrons in elements and compounds are often given nuclear data tables in different references.

The transmission of electrons emitted by a beta radioisotope source – beta particles is significantly different than the transmission curve of monoenergetic electrons because of the continuous distribution of beta particles energy. The low-energy beta particles are rapidly absorbed, however the main part the curve to have approximately exponential function. This exponential function has only empirical approximation and doesn't have a fundamental basis in physical processes, as it is a case for the exponential attenuation of gamma rays (next section). An *absorption coefficient* η is sometimes empirically defined by:

$$I = I_0 e^{-\eta x} \quad \textbf{(7)}$$

where I_0 is the initial intensity of beta particles and x is the absorber thickness in g/cm^2.

The *backscattering* is process of large-angle deflection where the incident electron significantly changes its direction, leaving the absorber.

This phenomenon is the most important for electrons with low incident energy and absorbers with high effective atomic number. This process can have a significant effect on the response of detectors.

1.3.3 Gamma ray interactions

There are three most important gamma ray interactions: *Compton scattering, photoelectric absorption,* and *pair production. T*hese processes lead to the significant change of the original gamma-ray photon, both of the movement angle and the energy.

1.3.3.1 Compton scattering of gamma photon

The Compton scattering is a scattering of the incident gamma ray photon and an electron in the absorbing material. In general case this is the dominant interaction for typical gamma-ray energies. In Compton scattering, the incident photon is deflected by angle θ with respect to its original direction (see Figure 1.6). The photon transfers a portion of its energy to the electron – so called *recoil electron*. All angles of scattering are possible; the energy transferred to the electron can vary from almost zero to a large part of the gamma-ray energy. The expression that relates the energy transfer and the scattering angle is given by the following equation:

$$h\nu' = \frac{h\nu}{1 + \frac{h\nu}{m_0 c^2}(1 - \cos\theta)} \qquad \textbf{(8)}$$

where h is the Planck constant and ν is the photon frequency. The probability of Compton scattering per atom number depends on available electrons i.e. with the atomic number Z. The differential cross-section of the scattered gamma photon is described by well-known Klein-Nishina formula:

$$\frac{d\sigma}{d\Omega} = Zr_0^2\left(\frac{1}{1+\alpha(1-\cos\theta)}\right)^2\left(\frac{1+\cos^2\theta}{2}\right)\left(1+\frac{\alpha^2(1-\cos\theta)^2}{(1+\cos^2\theta)(1+\alpha(1-\cos\theta))}\right) \quad \textbf{(9)}$$

where $\alpha = h\nu/m_0c^2$ and r_0 is the classical electron radius.

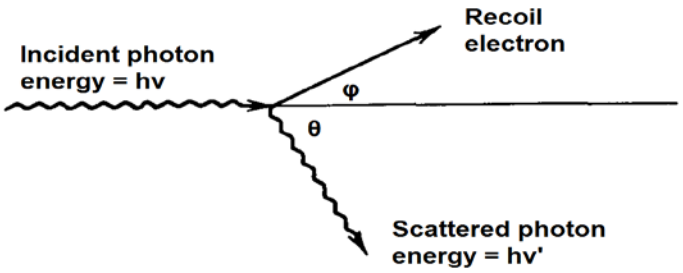

Figure 1.6: Schematics of Compton scattering

1.3.3.2 Photoelectric absorption

In this process a photon is literally absorbed by an atom and the energy is transferred to an ejected electron – *photoelectron* which is ejected by the atom from one of its bound shells, and in the process the photon completely disappears. The photoelectric absorption cannot take place with free electrons. The energy of photoelectron is given by:

$$E_{pe} = h\nu - E_b \quad \textbf{(10)}$$

where E_b is the binding energy of the (photo)electron.

After the emission, a photoelectron leaves ionized atom – with a vacancy in the shell from which the photoelectron is emitted. The vacancy is either filled from a free electron in absorber (if one exists) or by cascade of electrons from higher atomic shells. Each cascade produce a characteristic X-ray. This X-rays are in general reabsorbed in the absorber. In some cases an Auger electron is emitted instead of a characteristic X-ray i.e. energy of the relaxation of the electron filling the lower shell is transferred to an electron in the same atom, instead to a photon. The photoelectric absorption is becoming more dominant at lower energies and higher effective atomic number of the absorber.

1.3.3.3 Pair production

The pair production is an inverse process of electron-positron annihilation. The process becomes possible only if the gamma photon have energy of at least twice of electron rest mass – 1022 keV. However, the process becomes important for the energies of several MeV.

The process occurs in strong electromagnetic fields i.e. near to a nucleus. Due to this fact, the pair creation is more important for the absorbers with higher effective atomic number and roughly it is proportional to the square of the atomic number of the absorber. The positron created in the pair creation will most probably annihilate in the absorber, creating two photon of 511 keV and this process of pair creation – annihilation is very important in certain detectors.

The photoelectric absorbtion is predominant at low energies, Compton scattering is dominant at medium energies and the pair production is predominant at high energies (see Figure 1.7). ([1])

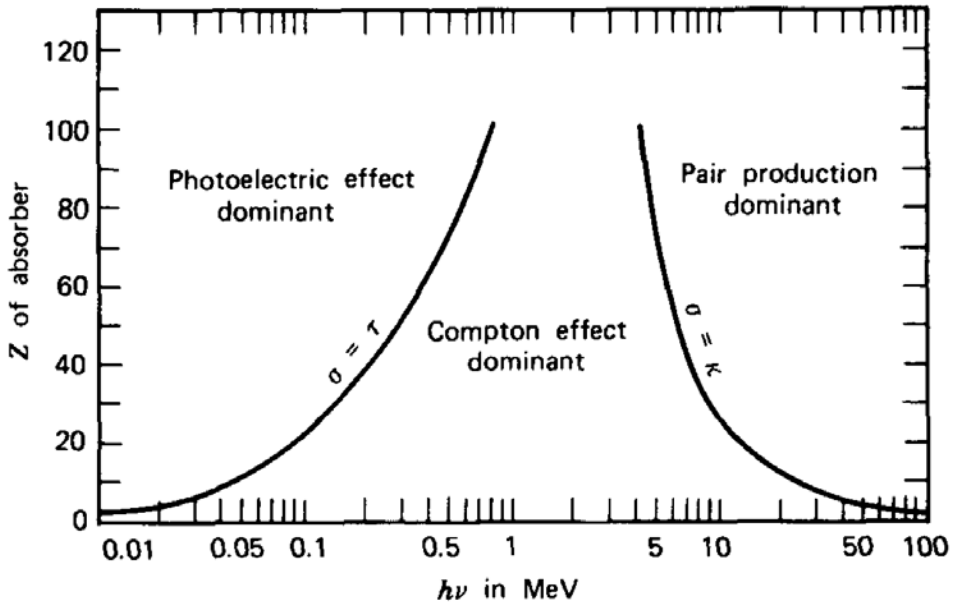

Figure 1.7: The relative comparison of the three major types of gamma-ray interaction depending on energy and the atomic number of absorber. The lines show the values of Z and hv for which the two effects are equal. (From The Atomic Nucleus by R. D. Evans. Copyright 1955 by the McGraw-Hill Book Company.) ([1])

1.3.3.4 Gamma-ray attenuation

When gamma radiation of intensity I_0 is incident on an absorber of thickness x the emerging intensity I after the absorber is given by the exponential function:

$$I = I_0 e^{-\mu x} \tag{11}$$

where μ is the attenuation coefficient. The attenuation coefficient is the sum of probabilities of gamma-ray removal per unit path length by three main processes:

$$\mu = (photoelectric) + (Compton) + (pair) \tag{12}$$

The attenuation coefficient is a inverse of mean free path which quantify the average distance which gamma ray pass before an interaction occurs:

$$\frac{1}{\mu} = \lambda = \frac{\int_0^\infty x e^{-\mu x} dx}{\int_0^\infty e^{-\mu x} dx} \tag{13}$$

Use of the linear attenuation coefficient suffers from serious drawback due the fact that it varies with the density of the absorber, even if the material is the same. Therefore, the mass attenuation coefficient is used defined as μ/ρ.

1.3.4 Radiation doses

The radiation is dangerous to living organisms and it is important to quantify the exposure to radiation and the permissible limits. For the purpose of radiation protection, dose quantities are expressed in three ways: absorbed, equivalent, and effective dose as it is shown on the Figure 1.8.

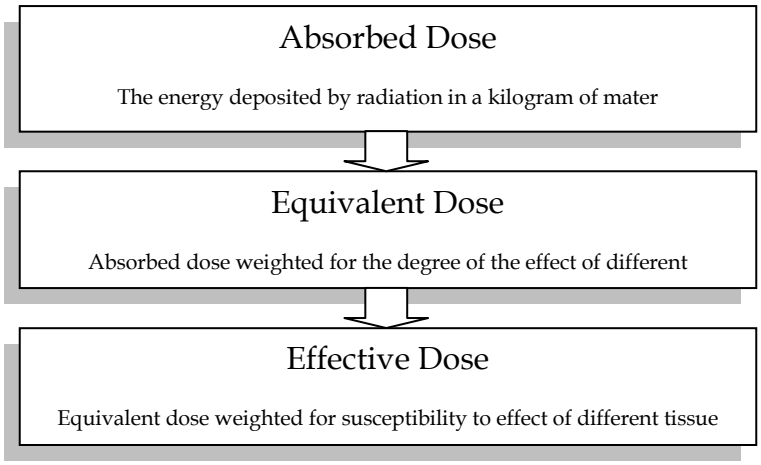

Figure 1.8: Relationship between effective, equivalent and absorbed doses

1.3.4.1 Absorbed dose

When ionizing radiation penetrates matter, it deposits energy along its path. The energy absorbed by an object from exposure to radiation is called an absorbed dose (D) and it represents a mean energy deposited in matter per unit mass. In the SI system of units, the absorbed dose is measured in joules per kilogram ($J\ kg^{-1}$) or specially named a unit the gray ($Gy = J\ kg^{-1}$). Old unit for absorbed dose was rad – a non-SI unit (100 rad = 1 Gy).

1.3.4.2 Equivalent dose

Different radiation types (alpha, beta or gamma) is absorbed in living matter will have different a biological effect. Effectively, 1 Gy of alpha radiation is much more harmful to any living tissue than 1 Gy of beta or gamma radiation. The equivalent dose (H) is obtained from the absorbed dose multiplied by the specific radiation weighting factor – w_R. Some values of w_R are presented in the Table 1.1.

Table 1.1: Radiation weighting factor for different radiation types ([2])

Radiation type	**Radiation weighting factor W_R**
Photons, all energies	1
Electrons, myons, all energies	1
Protons and charged pions	2
Alpha particles, fission fragments, heavy ions	20
Neutrons	A continuous function of neutron energy

The equivalent dose is expressed by a unit called the sievert (Sv) – 1 Sv = 1 Gy x w_R. Old unit for the equivalent dose was rem – 100 rem = 1 Sv. One mSv of α-particies produces the same effect as one mSv of γ's.

1.3.4.3 Effective dose

Different human tissues or organs have different radiation sensitivities. In principle, tissues which have higher cell reproduction rate are more sensitive. For instance, bone marrow and gonads are much more radiosensitive than muscle, brain or nerve tissue. Thus the effective dose gives an indication of how exposure can affect health it is obtained as the equivalent dose is multiplied by a tissue weighting factor w_T which represent sensitivity of given tissue or organ. The Table 1.2 ([3]) ([4]) shows some representative values of w_T for given tissue and organs. The unit used for effective dose is also the sievert.

Table 1.2: Tissue Weighting Factor, W_T ([3]) ([4])

Tissue	W_T
Gonads	0.20
Red bone marrow	0.12
Colon	0.12
Lung	0.12
Stomach	0.12
Bladder	0.05
Breast	0.05
Liver	0.05
Brain	0.05
Thyroid	0.05
Skin	0.01
Bone surfaces	0.01

1.3.5 Basic notions

1.3.5.1 Radioactivity unit

The radioactivity is defined as its rate of decay of a radioactive isotope and is given by the law of radioactive decay:

$$\frac{dN}{dt} = -\lambda N \,, \qquad \textbf{(1)}$$

where N is the number of radioactive atoms, λ is the decay probability and t is the time. The solution of this equation is:

$$N = N_0 e^{-\lambda t} \,, \qquad \textbf{(2)}$$

where N_0 is the the number of atom at t=0.

The SI unit of radioactivity is a Bq (Becquerel) which represents one decay per second. The historical unit of radioactivity was 1 Ci (Curie), 1 Ci = 3.7×10^{10} Bq = 37 GBq.

Often the term half-life is used to describe a radioactivity of an isotope. It represents a time needed to half of the atoms to decay in a given sample:

$$T_{1/2} = \frac{\ln 2}{\lambda} \quad \textbf{(3)}$$

1.3.5.2 Energy unit

The radioactive decay is an energy transformation and there is need to quantify the energetic result of decay. The traditional unit for a measurement of radiation energy is eV (electron volt) - as the kinetic energy gained by an electron by its acceleration through a potential difference of 1volt. More often keV and MeV are used. The SI unit for energy is joule – J, while the eV is not a SI unit: 1 ev = 1.602×10^{-19} J.

CHAPTER

2 Natural sources of radon and mechanisms of its release

Radon, with atomic number of 86 is the heaviest noble gas and thus chemically very inert. Due to its non-reactive nature and mobility it can migrate from the place of its origin and accumulate in indoor air. In this section: the physical properties and importance of radon, the sources of radon, mechanisms of its release, migration and accumulation in indoor air are described.

2.1 Discovery and importance of radon

Historically speaking, problem of radon originates from 15. century, although at that time it was still not discovered. Namely, at the end of 15. century, in silver mines in the region of Schneeberg in Saxony and Jachymov region in Czech a very high mortality among miners caused by lung diseases was found. This was first documented by Paracelsius in his book ([5]). At that time it was thought that main cause of lung diseases comes from inhaling ore dust that contains arsenic and various heavy metals. After more than 3 centuries, this disease was defined as a lung cancer (Haerting i Hesse, 1879) .

As mentioned in the first chapter, radium and polonium were discovered by Pierre and Marie Curie by extraction from the ore in Jachymov mine (Curie i Curie, 1898). A few years after, in year 1900, E.F. Dorn has discovered radon and has named it at first as the radon emanation (since it origines from radium). A year later, a high radon concentration has been measured in Schneeberg and Jachymov mines (Elster i Geitel 1901). Since at that time it was already known that skin cancer is related to gamma radiation coming from radium, it was assumed for the first time that high radon concentration is responsible for lung cancer.

It was not understood how radon itself can be related to lung cancer, since it is inert gas and practically all radon you inhale you exhale as well, until Bale proposed that a possible cause of lung cancer can be radon progenies (Bale, 1951). Afterwards, numerous measurements of radon and its progenies has been performed in mines and dwellings. Nowadays, World Health Organization has unambiguously established that radon is the second leading cause of lung cancer after cigarette smoking (WHO, 2005). In Table 2.1, annual average doses of exposure from natural and artificial sources is given.

Table 2.1. Annual average doses (mSv) of ionizing radiation by different sources

Source of radiation	Worldwide annual average dose (mSv)
Inhalation (radon gas)	1.26
External terrestrial	0.48
Ingestion	0.29
Cosmic radiation	0.39
Medical diagnosis	0.6
Other artificial sources	<0.012

Considering that radon and its progenies are one of the leading cause of lung cancer and that they contribute with more than 50% to total population exposure it is important to understand its origin, transport and accumulation in dwellings in order to reduce population exposure.

2.2 Properties of radon

2.2.1 Radioactive decay chain

Up to now, it has been produced and identified 39 radioactive isotopes with atomic masses ranging from 193 to 231 [http://www.nndc.bnl.gov/ensdf/]. Among them, there are only three naturally occurring isotopes. Those three originate from different natural decay series: ^{219}Rn (colloquially known as actinon) originates from actinium decay series (^{235}U), ^{220}Rn (thoron) originates from thorium decay series (^{232}Th) and ^{222}Rn (radon) originates from ^{238}U decay chain. In Figures 2.1 and 2.2 are presented natural decay series of ^{238}U and ^{232}Th.

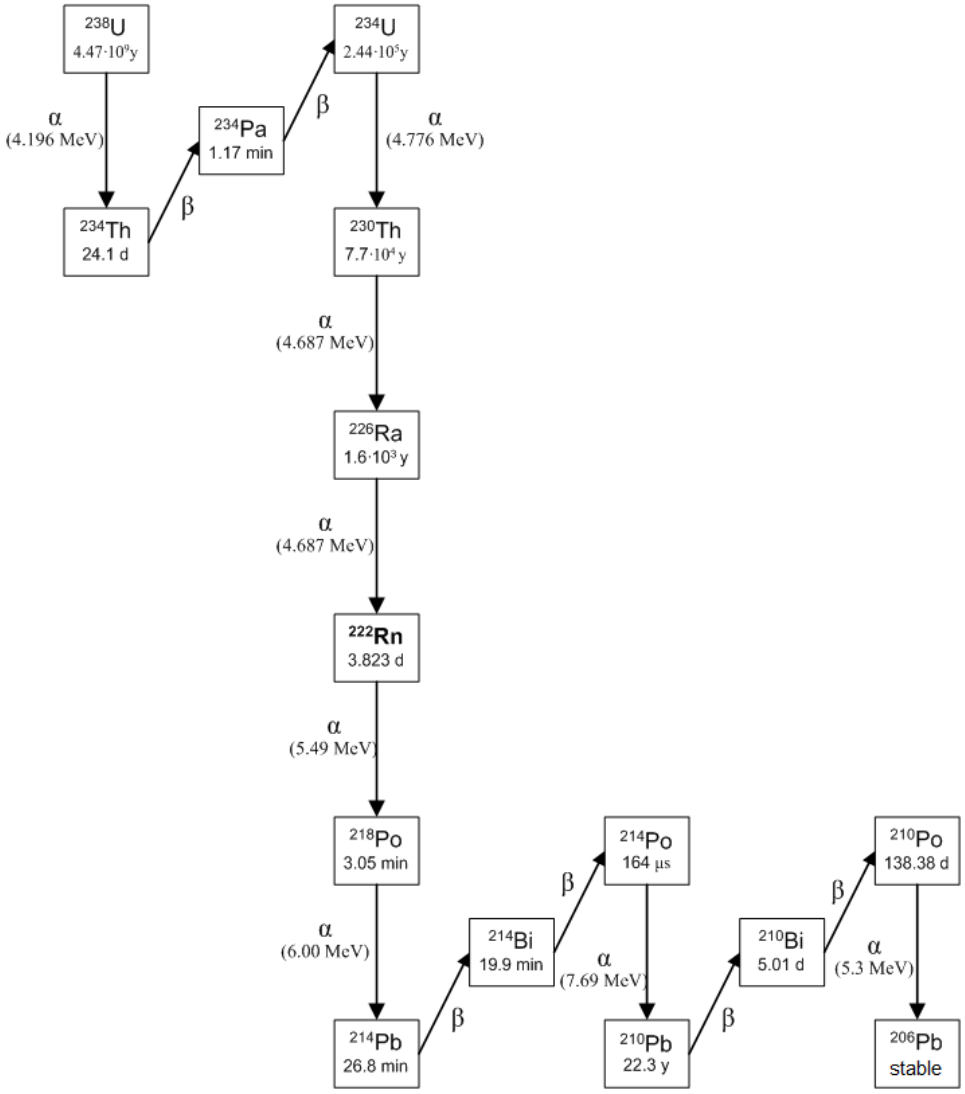

Figure 2.1 Natural decay series of ^{238}U: the source and decay products of ^{222}Rn

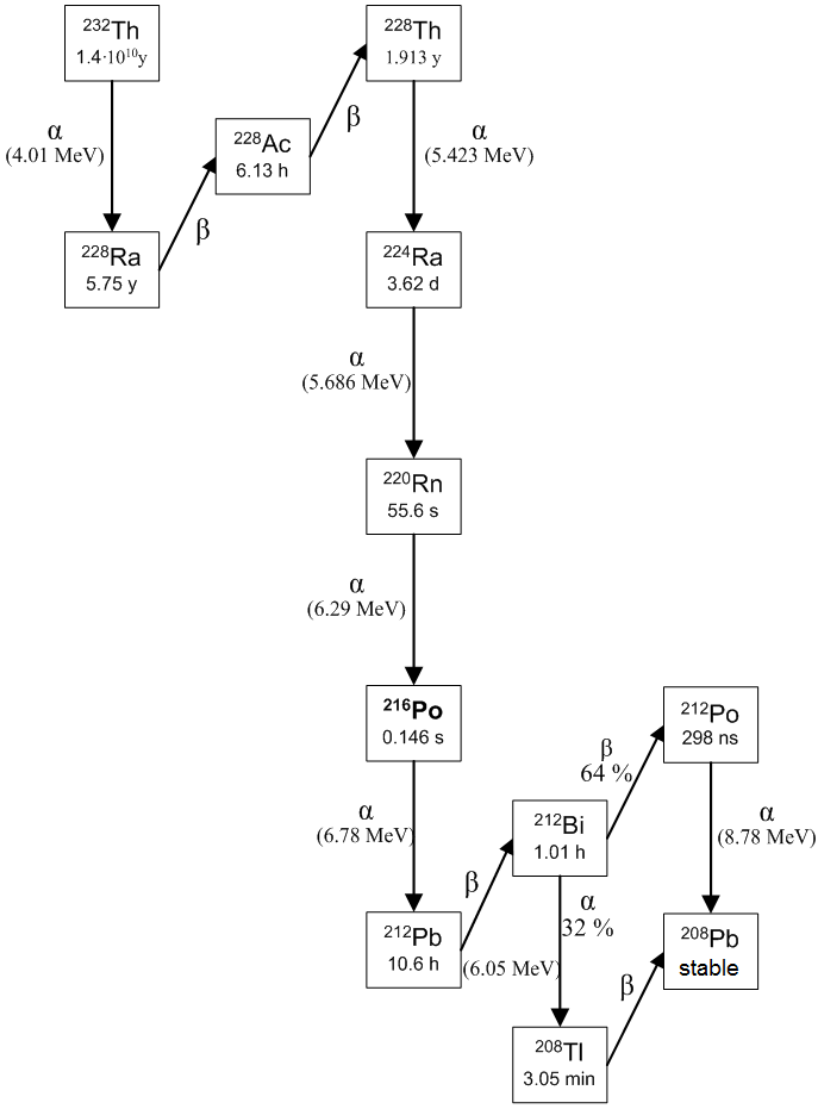

Figure 2.2 Natural decay series of ^{232}Th: the source and the decay products of ^{220}Rn

2.2.2 Importance of radon

The relative importance of Rn isotopes depend on their half-lives and abundances. The ^{219}Rn is practically ignored since it is the shortest lived, with the half-life of 5.71 s and it is always present into small amounts compared to ^{222}Rn ($T_{1/2}$ = 5.51 d), since natural abundance of uranium is 99.28% ^{238}U, 0.714%, ^{235}U i 0.0058% ^{234}U. The half-life of ^{220}Rn ($T_{1/2}$ = 55.6 s) is much shorter compared to the half-life of ^{222}Rh and

therefore a distance that ^{220}Rn diffuses is much shorter compared to ^{222}Rn, making ^{222}Rn the most dominant isotope. Nevertheless, in nature there are regions that have very high Th/U ratio {Kerala, India] and consequently very high thoron concentration, that has to be taken into account for the estimation of health hazard.

The radon itself is not of primarily concern for health effect, since radon is a noble gas and due to its half-life, the most of radon that has been inhaled will be exhaled as well. The major concern is due to the short-lived progenies (^{218}Po, ^{214}Pb, ^{214}Bi, ^{214}Po; see Fig. 2.1 for ^{222}Rn) that are alpha and beta decaying nuclei. They are chemically active and being charged they tend to attach to air particles. In this attached phase, they can stick on epithelial tissue of lung and shortly decay afterwards (from 0.2 ms to less than 27 minutes). In such a short way, bronchi are irradiated by strongly ionizing alpha particles not giving enough time for lungs to sweep them away. From now on, we will refer to ^{222}Rn as radon.

2.2.3 Sources of radon

Radon origins from the direct decay of ^{226}Ra, which is one of the progenies in the 238U chain. Therefore, radon which is formed in rocks and soil primarily depends on radium concentration and subsequently on uranium concentration in rocks and soils. Since uranium is litophile element, it predominantly appears in magmata rocks rich in silica such as granites and syenites, and vulcanic rocks such as rhyolite and porphy. Uranium concentration varies significantly in different minerals ranging from quartz having weighted fraction of less than $3 \cdot 10^{-12}$ up to UO_2 with weighted fraction of 0.88 ([6]). Mineral oxides in general have a higher uranium concentration then the minerals themselves. Furthermore, it was found that within the same type of minerals, such as zircon, U concentration varied from 1-10 ppm in one and 800-4000 ppm in a second zircon ([7]).

Soils are formed from bedrocks that have been exposed to different processes such as chemical and mechanical weathering, crushing from land ice. They can be

formed as eruption products from volcanoes, precipitation products from sea and fresh water, and finally loose soil is transported and redeposited by water and/or wind...

As a result of soil formation by means of abovementioned processes, uranium and radium concentrations differs between soils and bedrocks. In Table 2.2 are given typical ranges of radium concentrations in some common rocks and soils.

Table 2.2. Typical ranges of radium concentrations in some common rocks and soils

Rock	^{226}Ra (Bq kg^{-1})	Soil	^{226}Ra (Bq kg^{-1})
Granite, normal	25 - 80	Till, with normal Ra content	15 - 65
Granite, uranium rich	100 - 500	Till, with fragments of granite	130 - 125
Sandstone	1 - 60	Till, with fragments of U-rich granite	125 - 360
Limestone	5 - 40	Gravel	30 - 75
Shale	10 - 125	Sand	5 - 35
Black shale	10 - 2000	Silt	10 - 50
Alum shale	125 - 4300	Clay	10 - 100
Uranium ore	12000 - $2.5 \cdot 10^5$	Soils with fragments of alum shale	175 - 2500

Uranium and radium have different chemical properties and therefore are affected in a different ways by chemical etching and weathering. Uranium is easily transported and precipitated in permeable structures like fissures usually in reducing environment. Transport of uranium, that was once precipitated in reducing

environment, by ground water can lead to large deposit of uranium ore. On the other hand radium is much less mobile than uranium since it usually forms phosphates and carbonates that are not easily dissolved. In contrast to uranium, there are no radium minerals or minerals of its progenies, so even the highest concentration of uranium minerals do not contain more than $2.5 \cdot 10^{-5}$ % of radium. Due to large solvability of uranium compounds in water and its migration toward large water basins, there is no equilibrium between uranium and radium.

Besides natural sources of radon, there are anthropogenic sources as well: debris from uranium and phosphate mines. These locations can release up to 20% of radon formed in mines and radon can escape with a rate of 37 $Bqm^{-2}s^{-1}$ ([8]). Ashes from the coal burning power plant, can also increase radon concentration in air, but their contribution is negligible.

2.2.4 Radon emanation

Radon is formed when radium decays by alpha particle. This alpha decay can be presented in the following form:

$$^{226}Ra \rightarrow ^{222}Rn + \alpha$$

According to linear momentum conservation law, with the alpha particle ejected with 4.78 MeV, radon will recoil with energy:

$$\left.\begin{aligned} E_\alpha &= \frac{m_{Rn}}{m_{Rn}+m_\alpha}Q = \frac{A-4}{A}Q \\ E_{Rn} &= \frac{m_\alpha}{m_{Rn}+m_\alpha}Q = \frac{4}{A}Q \end{aligned}\right\} \Rightarrow E_{Rn} = \frac{4}{A-4}E_a = 86keV$$

The range of radon with this recoil energy is of the order of tens of nm. Some typical ranges are: from 20-70 nm for mineral grains of average density (34 nm for quartz), 77 nm in water and 53 μm in air (Ziegler et al, 1985). The recoil of radon is considered as the main process that enables radon to leave a mineral grain (Fleisher 1980). Radon can also leave a mineral grain by diffusion, but this process is negligible

since the radon diffusion coefficient in mineral grains is very low (10^{-31} - 10^{-69} m^2s^{-1}), which corresponds to small diffusion lengths (10^{-13} - 10^{-32} m) ([9]) ([10]).

The process in which radon is released from a mineral grain into a pore space between grains is defined as emanation. The fraction of released radon atoms compared to the total number of created radon atoms within a grain is defined as emanation fraction or emanation factor.

In Figure 2.3. different scenarios of radon transport from its origin in a mineral grain till it stops or releases from a mineral grain are illustrated.

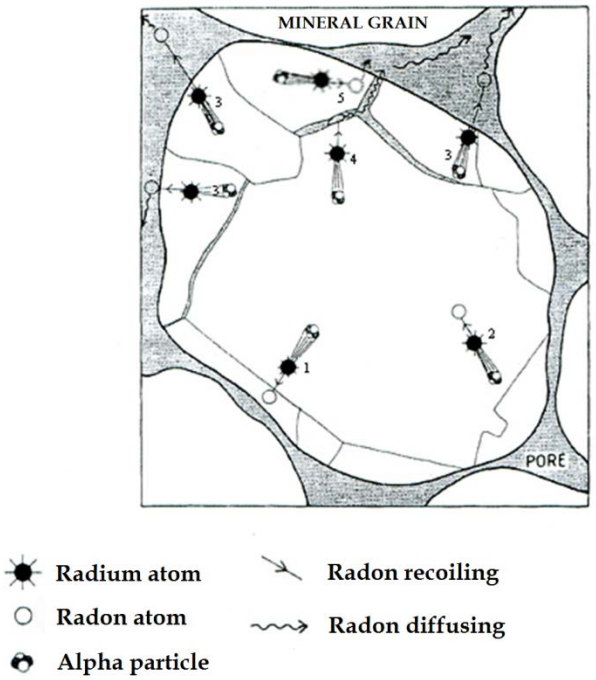

Figure 2.3. The scenarios of radon transport within the mineral grain and the means of emanation.

Depending on the place of origin of radon in grain and direction of its recoil, a several scenarios are possible:

1. Radium atom decays near the surface of crystal and recoiling radon has enough energy to leave crystal, traverse through pores between crystals and gets attached to the adjacent crystal.

2. Radon atom was created deep in a crystal and its decay orientation is such that radon is completely stopped in the crystal
3. Radon originates near the surface of crystal and by recoil it reaches a pores between crystals and further continues by diffusion.
4. Due to recoil, radon reaches to micro-fissures in a crystal, where it continues by diffusion reaching the pores and thus leaving the crystal
5. Due to recoil, radon stops near the crystal surface and continues to move by diffusion and eventually leaves the grain and reaches the interstitial place

Radon emanation can also takes place by means of water leaching which drains radon through the radiation damages in crystals ([11]) ([12]).

2.2.5 Physical radon emanation factors

There are numerous factors that influence radon emanation and they can be grouped in experimental factors. Some of the experimental factors are: instrument properties and environment, sample properties and environment, definition of radon emanation and they will not be further explained. The most important physical factors are: distribution within the grains, a size and shape of grain, moisture content in material, temperature, outer and inner size of pores, existence of micro-fissures etc. ([13]).

If ^{226}Ra is distributed on a grain surface, radon concentration will be proportional to the surface of the grain. On the other hand if radium is uniformly distributed inside the grain, radon concentration will be inversely proportional to the diameter of the grain (assuming spherical grain shape). And thus, for spherical grains of 10 μm in diameter, radon emanation fraction is 2 orders of magnitude higher if radium concentration is distributed on the grain surface, than if radium is uniformly distributed ([13])

The emanation factor is decreasing with the grain size, since for larger grains, there is smaller probability that radon can by recoil leave the grain. In Table 2.3 are given grain size for typical types of soil, and emanation factor for different soils and rocks.

Table 2.3. Typical ranges of radium concentrations in some common rocks and soils

Type of soil	Grain size (μm)	Soil type	Emanation factor (%)
Fine clay	< 0.6	Clay	30 - 70
Coarse clay	0.6 - 2		
Silt	2 - 60		
Sand	60 - 2000	Sand	15 - 30
Gravel	2000 - 60000	Gravel	15 - 40
		Crushed U-rich granite (1-8 mm size)	15 - 30

While large emanation factor of clay is obviously due to small size of its grains, the large emanation of gravel is not possible to explain by the size of grains. It was found that radium atoms in gravels have been absorbed in the fine fractions of soil and also that radium atoms have been precipitated on the surface of grains which are the processes that increase emanation (Ek and Ek, 1995). In addition, for the higher porosity of soils and rocks the emanation is higher since the radon diffusion is larger.

The moisture content in the pores between the grains and in the fissures increase the emanation factor. Namely, due to much greater stopping power of water compared to air, radon emanating from one grain into the pores, has much higher probability to remain in pore space if it is filled with water than if it is dry. The range of recoiling radon atoms in air is around 60 μm and therefore radon atom has a higher probability to attach to adjacent soil grain. The emanation factor is increasing with increasing water

content, until it reaches saturation. Afterwards, the emanation factor tends to decrease due to smaller diffusion coefficient in water than in air ([13])

It was shown by Istandar et al, that emanation factor linearly increases with temperature (Istander, 2004) since with higher temperature physical adsorption of radon on mineral grains decrease. On much higher temperature, of several hundreds of °C, diffusion length of radon in mineral grains increases significantly and consequently increasing the radon emanation.

2.3 Radon transport

After radon has emanated from mineral grains, it can further travel by means of diffusion and advection. With convection, radon can travel large distances since it can be guided by forced flow of ambient gases such as CO_2 and CH_4.

2.3.1 Transport by diffusion

The primary means of radon transport is chaotic molecular motion with tendency to move from the region with higher concentration, toward the region of lower concentration. This tendency is described by Fick's law saying that the diffusion flux of fluid is proportional by the gradient of concentration of that flux:

$$\vec{J}_d = -D_e \nabla C \qquad (4)$$

where: $\vec{J}_d$ is the radon flux density vector (Bq m^{-2} s^{-1}); D_e is the effective diffusion coefficient (m^2 s^{-1}); C is the radon concentration in the environment (Bq m^{-3}). Effective diffusion coefficient, also called "interstitial" is defined as the ratio of flux density in air pores of given matrix and the gradient of the radon concentration in air-filled pores. The upper value is the radon diffusion coefficient in air. In literature is also used bulk

diffusion coefficient that is defined as the ratio of flux density and radon concentration gradient through the whole geometry of the matrix and only from the air pores:

$$D = \varepsilon D_e \qquad (5)$$

where, porosity of the environment ε is taken into account. Since radon concentration in pores filled with water air are not the same in more general case it is necessary to change porosity parameter ε with $\varepsilon_a + K_T \varepsilon_w$, where ε_a and ε_w are porosities fractions is air and water respectively, while K_T is the ratio between the number of radon atoms in water and in air.

In table 2.4, some typical radon diffusion coefficients are given. As can be seen from the table 2.4, radon can diffuse as easily through the soil with large grains (such as gravel and large sand) as through the air. On the other hand, diffusion coefficient in water is 4 orders of magnitude lower than the diffusion coefficient in air. Therefore, diffusion length (defined as $L = \sqrt{D / \lambda_{^{222}Rn}}$) in water is two orders of magnitude smaller than diffusion in air and thus can be neglected.

Table 2.4. Radon diffusion coefficients D ($m^2 s^{-1}$) in different media (UNSCEAR, 1988)

Medium	D ($m^2 s^{-1}$)	L (m)
Air	10^{-5}	
Boulders -coarse gravel	10^{-5} - $5 \cdot 10^{-6}$	
Dry sand	10^{-5}	
Moist sand	$2.5 \cdot 10^{-6}$	
Till	$5 \cdot 10^{-7}$ - $2.5 \cdot 10^{-7}$	
Clayey till	$8 \cdot 10^{-8}$	
Water	10^{-9}	

The diffusion length or mean diffusion distance given in table 2.4 indicate that, assuming diffusion transport only, radon can reach house foundation only for soil located one or two meters beneath the foundation.

2.3.2 Transport by advection

For the fluids that have Reynolds number smaller than around 4, which is the case for radon transport through the soil and building material, the air flow can be described by Darcy's law:

$$q = -\frac{k}{\mu}\nabla P \qquad (6)$$

where: q - is the Darcy's velocity vector (m s^{-1}) defined as the flux per unit area over the element of volume large to the individual pores, k - is the gas permeability through the soil (m^2), P - is the pressure (Pa), μ - is the dynamic viscosity (Pa s). It describes fluid dynamics through the porous medium as a function of pressure gradient. The pressure difference is the most often caused by meteorological conditions, ventilation and heating systems. Finally, radon flux density can be expressed as:

$$J_a = Cq = -\frac{Ck}{\mu}\nabla P\,. \qquad (7)$$

Very important parameter that influence radon flux is the soil gas permeability since it can differ up to 10 orders of magnitude for different type of soils (from 10^{-7} for clean gravel up to 10^{-16} for fine clay). In addition, soil are not homogeneous, so in general permeability can differ for different directions and furthermore, porosity is time dependent due different dynamical processes (weathering, forming of fractures...).

The direction of radon flux is changed in opposite direction with a change of barometric pressure, and thus decrease of barometric pressure tends to increase air flow from soil (including radon) to atmosphere while increase of barometric pressure tends to suppress air flow from soil to atmosphere. ([14])

in general permeability.

2.3.3 General transport equation

In general case, radon transport equation should include transport doe to diffusion and advection, emanation of radon from the mineral grains and its decay. Water content can influence diffusion coefficient, permeability and in general radon concentration is spores filled with air and water are different. From the abovementioned, transport equation can be expressed as: ([9])

$$\frac{1}{\varepsilon}\frac{\partial(C_a\varepsilon_a + C_w\varepsilon_w)}{\partial t} = D_e^{'}\nabla^2 C_a - \frac{k'}{\mu}\nabla P\nabla C_a + \frac{1-\varepsilon}{\varepsilon}\rho\lambda E' - \frac{\lambda}{\varepsilon}(C_a\varepsilon_a + C_w\varepsilon_w) \qquad (8)$$

where:

ε_a, ε_w - is the porosity of air and water defined as the ratio between volume of pores filled with air (water) and total volume of medium ($\varepsilon = \varepsilon_a + \varepsilon_w$); λ - is the radon decay constant; C_a, C_w - are the radon concentrations in air- and water-filled spores; ρ - is the density of mineral grain; E - is the emanation rate; Prime symbol ' indicates that parameter value is water dependent the rest of the parameters are previously defined. Diffusion through the water is neglected.

From the general transport equation and due to the large differences in permeability of several orders of magnitude for different soil, it is clear that diffusion is dominant in low permeability environment, while in high permeability environment dominates transport by advection. The limit between these two processes is set around 10^{-11} m^2 ([15]).

In case that diffusion is dominant means of transport, 1D transport equation in air for steady state is given by:

$$D_0\frac{d^2C}{dx^2} - \lambda C = 0 \qquad (9)$$

whose solution is:

$$C = C_0 e^{-\frac{x}{L_d}} \qquad (10)$$

where: $L_d = \sqrt{\frac{D_0}{\lambda}} = \sqrt{D_0 \tau}$ is the diffusion length in air

Similarly, transport equation assuming dominant advective motion with constant Darcy's velocity (q=const) in a steady state reduces to:

$$q\frac{dC}{dx} + \lambda C = 0 \qquad \textbf{(11)}$$

whose solution is:

$$C = C_0 e^{-\frac{x}{L_a}} \qquad \textbf{(12)}$$

where $L_a = \frac{q}{\lambda}$ is the advective length is the air.

Finally, in the case when both diffusion and advection are relevant means of transport, the solution for 1D steady state is given by following formula:

$$C = C_0 \left\{ 1 - \exp\left[\frac{1}{2L_d^2}\left(L_a - \sqrt{L_a^2 + 4L_d^2} \right) x \right] \right\} \qquad \textbf{(13)}$$

assuming that outdoor radon concentration is 0 Bg/m^3 which is reasonable assumption since radon concentration in soil gas is a few orders of magnitude higher that outdoor concentration, and thus can be neglected.

For this combined effects of radon transport, one can estimate a distance that radon can travel for which it's concentration will be reduced by factor (1-e^{-1}). This distance is defined as the "migration distance" and is given by following formula:

$$M_d = \frac{1}{2}\left(L_a + \sqrt{L_a^2 + 4L_d^2} \right) \qquad \textbf{(14)}$$

2.4 Radon in buildings

Radon is always present in air due to its continuous release from soil. Under certain conditions, radon concentration can build up in closed buildings and indoor concentrations can be much higher than outdoor radon concentrations. Radon

concentration in buildings depends not only on radon (and radium) concentration in soil beneath and building materials, but on the construction of buildings as well and residents' habits.

2.4.1 Mechanisms of radon entry in buildings

In Figure 2.4, the means of radon entry from a soil and a building material is presented.

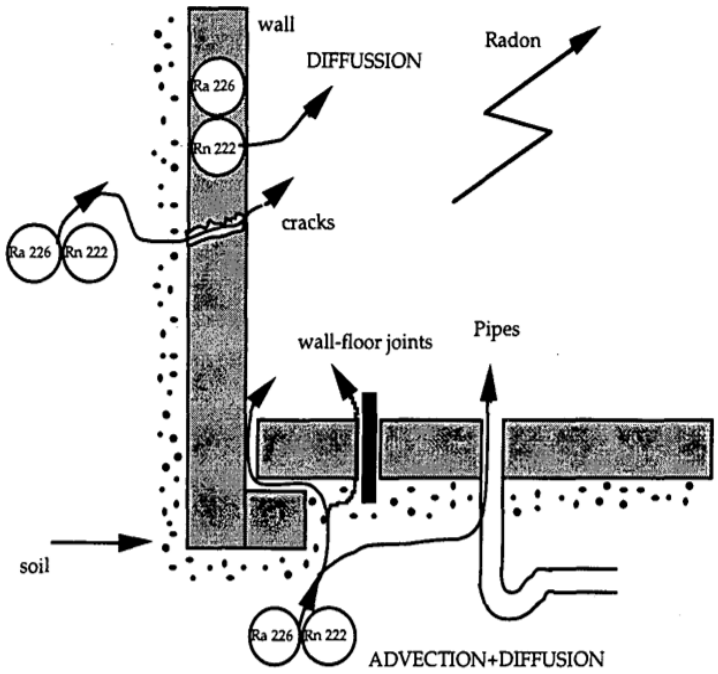

Figure 2.4 Mechanisms of radon entry in buildings from soil and building materials

In general radon entry in houses can be classified in tree group:

- radon entry from soil: diffusion and advection
- radon entry from building materials: diffusion
- radon entry from water supplies

2.4.1.1 Radon entry from soil

It was shown that concrete, which is usually used for building material or for foundation, has very low permeability factor ([16]) and thus it was assumed that the main source of radon entry from soil is by diffusion driven by difference in radon concentration is soil (of the order of tens of kBg m^{-3}) and indoor (of the order of a few tens of Bq m^{-3}).

It was found that indoor pressure is smaller by a few Pascals than outdoor or soil pressure due to various factors such as: wind, indoor-outdoor temperature difference, fans and heating systems... This small under-pressurization drives the advective flow from soil to indoor air. Since concrete is impermeable for radon, transport occurs through cracks in foundation and walls, wall-floor joints, along the water and electricity pipes and this contribution to indoor radon concentration could be even dominant one.

2.4.1.2 Radon entry from building material - Exhalation

Since most of the building materials has very small permeability, the diffusion is a dominant transport mechanism of radon through the building materials and with including the radon generation term, ([9]) radon transport in building material can be written as:

$$D_m \frac{d^2 C_m}{dx^2} - \lambda C_m = -G_m \qquad (15)$$

where: C_m is the radon concentration in pores of material, D_m is the diffusion constant of radon in material, and G_m is the radon generation term $G_m = \frac{A_{Ra} \rho_m f_m}{\varepsilon_m} \lambda$ that takes into account Ra concentration in material (A_{Ra}), its density (ρ_m) and porosity (ε_m), and emanation coefficient (f_m) and radon decay constant (λ).

From previous equation, using the boundary condition that Rn concentration is 0 Bq m^{-3}, at the surface of building material, radon distribution in pores of material can be derived as:

$$C_m(x) = \frac{A_{Ra}\rho_m f_m}{\varepsilon_m}\left[1 - \frac{\cosh(x/L_m)}{\cosh(d_{1/2}/L_m)}\right]$$

where $d_{1/2}$ is the half width of the material thickness and x is the distance from the centre of building material.

The rate at which is radon released from the building material by unit time is defined as the exhalation rate. For compact material, surface exhalation rate is used which is defined as the exhalation rate by unit surface (Bq m^{-2} s^{-1}), while for powdered (grained) material mass exhalation rate is used (Bq kg^{-1} s^{-1}). Therefore, exhalation rate can be derived from Fick's law, in which diffusion is corrected by the porosity factor, in order to express exhalation per unit volume:

$$E = -D_m \varepsilon_m \left.\frac{dC_m}{dx}\right|_{x=d_{1/2}} \quad (16)$$

and assuming that radon concentration at the surface of material is 0 Bq m^{-3}, exhalation rate is:

$$E = \lambda A_{Ra}\rho_m f_m L_m \tanh\left(\frac{d_{1/2}}{L_m}\right) \quad (17)$$

There are various techniques to measure radon exhalation rate, and since this is the aim of this thesis, they will be described in the following chapters.

2.4.1.3 Radon entry from water supplies

One of the minor sources of indoor radon is water supply. Usually this contribution is very small since water travels large distances from water cleaning stations to homes and thus the most of the radon decays along the path. More important contribution to indoor radon concentration could be in houses with private wells which are practically closed systems, from the water in a drained hole to water pipes in dwellings. Radon is easily released from water by water bubbling, so the highest contribution is coming from taking a shower or laundering. It is estimated that with radon concentration of 1 $kBql^{-1}$, indoor radon concentration will be increased by 100 Bq m^{-3} ([17]).

2.4.2 Ventilation: reducing radon concentration

Up to now, only mechanisms that led to accumulation of radon in building are discussed. The only natural way to reduce the indoor radon concentration is by ventilation which is by definition exchange of indoor air with outdoor air. Since outdoor radon concentration is usually smaller than indoor one, ventilation will cause reduction of indoor radon concentration. The ventilation rate is defined as the number of exchanges of indoor air per unit time (h^{-1}) and typical value is between 0.2 and 2 h^{-1} ([2]) ([8]). Beside natural air exchange, ventilation can be artificial as well (heating system, air conditioners...) and it such cases, ventilation rate can be even one order of magnitude higher.

2.5 Indoor radon concentration

As described in previous sections, indoor radon concentration depends on radon entry rate from soil, building material and water, while its reduction depends on the ventilation rate. Finally, by combining all effects, indoor radon concentration can be described by following equation:

$$\frac{\partial C}{\partial t} = G_s + \frac{E_b S_b}{V} - (\lambda + \lambda_v)C + \lambda_v C_{out} \qquad (18)$$

where: G_s is the volume radon entry rate from soil (Bq m^{-3} h^{-1}), E_b is the surface radon exhalation rate (Bq m^{-2} s^{-1}), S_b and V are the surface of building material and air volume in a room, λ_v is the ventilation rate (h^{-1}) and C_{out} is the outdoor radon concentration.
with the solution:

$$C(t) = \frac{G_s + \frac{E_b S_b}{V} + \lambda_v C_{out}}{(\lambda + \lambda_v)}\left(1 - e^{-(\lambda+\lambda_v)t}\right) \qquad (19)$$

As already discussed, the indoor radon concentration depends on numerous factors such as: radium concentration in soil and building material, emanation factor, porosity, permeability, types and designs of dwellings, inhabitants habits... Since these

factors are multiplicative in general, indoor radon concentration can be described as $R_i=R_o+ A*B*C...$ where R_i and R_o are indoor and outdoor radon concentration, while A,B,C... are above-described factors affecting radon concentration...

If we put equation under logarithm, it becomes: $\ln(R_i-R_o)=\ln(A)+\ln(B)+...$ Since $\ln(R_i-R_o)$ follows normal distribution, it is said that (R_i-R_o) follows log-normal distribution.

In the following section different radon measurement techniques are described.

CHAPTER

3 Radon measurement

Radon is the only alpha—emitting natural radioactive gas. There are three natural isotopes of radon: ^{222}Rn, ^{220}Rn and ^{219}Rn. They are often colloquially called "radon", thoron (Tn) and actinon (An). This means that the term "radon" in principle refers to ^{222}Rn. Actinon has a too short half-life of few seconds to be of any interest for the investigation.

Radon and several of its daughters decay away by emitting α particles (^{218}Po and ^{214}Po), β particles (^{214}Pb, ^{214}Bi, ^{210}Pb and ^{210}Bi). These β emitters also emit characteristic γ rays. This means that radon detection and therefore the measurement can be performed by detection of α, β and γ rays. Principally, the alpha radioactive radon progenies, ^{218}Po and ^{214}Po, are responsible for most of the radiation dose delivered by radon.

However, radon gas concentration is generally considered a good representative of the radon progenies concentration. Moreover, radon gas measurements are preferred because they are simpler to conduct and also they have a good cost-effect ratio.

The most widely used devices for radon measurement and their characteristics are shown on the Table 3.1: solid state nuclear track detectors (SSNTDs) i.e. alpha-track detectors (ATDs), electret ion chambers (EICs), activated charcoal detectors (ACDs), electronic integrating devices (EIDs) and continuous radon monitors (CRMs). Passive devices do not need electrical supply, while active devices require supply, but they can record the radon concentration fluctuations during the measurement period. The most common radon measurement in indoor air of homes is performed by ATDs, as they are cheap, easy to deploy and they are often use in the exposures for a one year period. The EICs are used for shorter measurement periods of few days up to few weeks (although in some cases it can be exposed for one year). The both of these device types are integrating the radon concentration during their exposure. CRMs can measure the variation of radon concentration and their use becomes more common as the price of these detectors has slowly declined.

Table 3.1: Radon gas measurement devices

No	Detector Type	Passive/ Active	Typical Uncertainty [%]	Typical Sampling Period	Cost
(1)	Solid State Nuclear Track Detectors (SSNTD), also Alpha Track Detectors	Passive	10 – 25	1 – 12 months	Low
(2)	Activated Charcoal Canisters	Passive	10 – 30	2 – 7 days	Low
(3)	Electret Ion Chamber	Passive	8 – 15	5 days – 1 year	Medium
(4)	Electronic Integrating Device	Active	~25	2 days – 1 year	High
(5)	Continuous Radon Monitor	Active	~10	1 hour – year(s)	High

3.1 Radon measurement techniques and devices

There are many techniques available for radon measurements and they are mainly divided in two fields of investigation: health physics and geosciences. Principally, the radon measurements are motivated by the possibility that cancers of different types might be induced by exposure to radon. In the second case, radon measurements range from mineral prospecting to geothermal studies and predictions of volcanic eruptions and earthquakes.

There is a dozen of important radon measurement techniques:

- solid scintillation
- liquid scintillation
- nuclear emulsion
- adsorption
- gamma spectrometry
- ionization chamber
- surface barrier detectors
- beta monitoring
- solid state nuclear track detectors (alpha track detectors)
- electrometer

- theromoluminiscent phosphors
- electret.

Often a device uses a certain technique and it is classified accordingly. The mentioned techniques can be performed both in laboratory and in field measurements.

3.1.1 Alpha track detectors

Polymeric plastics are the most widely used alpha track detectors in all fields except in high temperature environment and they are very often used in radon measurements, but also in neutron monitoring, experimental nuclear physics, space research, etc. They are simple, have a small size which makes them easy to manipulate and to deploy and also they are able to integrate the response over long periods of time.

An ATD is a small piece of a special plastic enclosed in a diffusion chamber that prevents the entry of radon decay products as shown in Figure 3.1. The plastic is in principal made of three types of polymers: a polyallyl diglycol carbonate (PADC or CR-39), cellulose nitrate (LR-115), or polycarbonate (Makrofol) material.

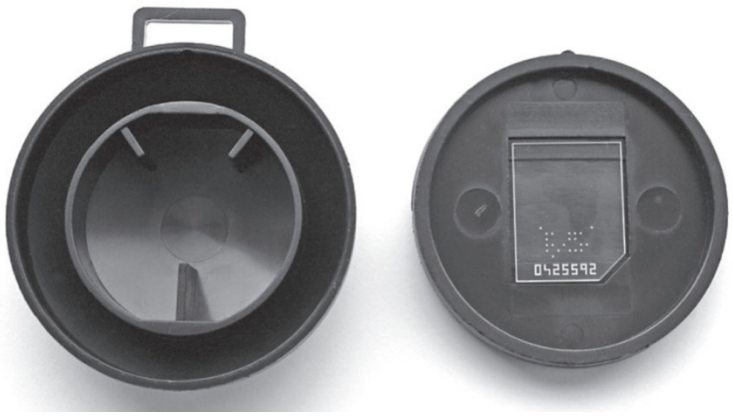

Figure 3.9: Example of an alpha track detector enclosed in a diffusion chamber

3.1.1.1 Principles of track formation

The polymers are sensitive to heavy charged particles, but not to beta particles, nor to gamma rays. The heavy particle leaves latent track - damage in dielectric media of breaks of polymer chains along its path (Figure 3.2). The latent tracks are relatively stable under usual conditions, although in some polymers they can sustain higher temperatures. The most damage is produced at Bragg peak and therefore the latent track is most resistant at that position. The diameter of the latent tracks is of order of tens of nm.

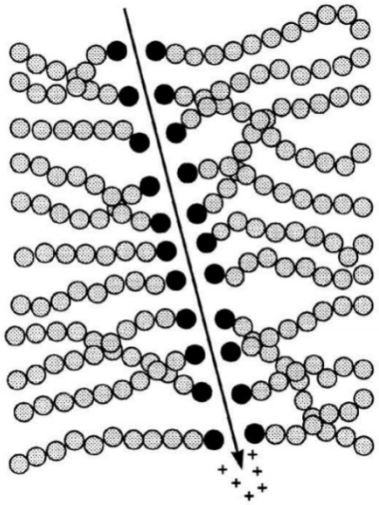

Figure 3.10: The latent track of heavy charged particle consists of polymer chain breaks along the path of the particle

The density of latent tracks is proportional to the exposure to heavy charged particles, for instance to radon and its progenies. The latent tracks are visible only by transmission electron microscopy and they are not easy to count and to estimate their density. Therefore, they are etched by a suitable etchant, in case of plastics the etchants are alkali NaOH or KOH. The etching enlarges the latent tracks, making them visible by microscope, but also fix them making them stable and permanent - Figure 3.3 (a). During the etching the etching speed of latent track V_T is higher than the etching speed of the surface (bulk) – V_B. The ratio of these speeds defines the "critical angle" , above which one the latent track will not become the permanent one (see Figure 3.3 (b)):

$$\theta_c = \sin^{-1}\left(\frac{V_B}{V_T}\right) \qquad \textbf{3.1}$$

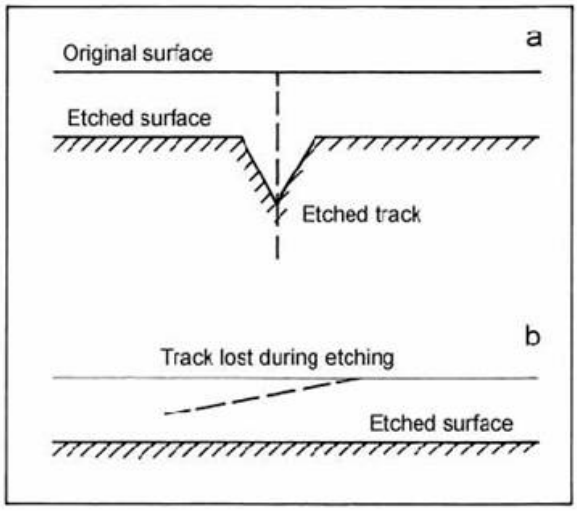

Figure 3.11: The process of the track etching in an ATD. The latent track (dash line) is enlarged by the etchant and the surface is also etched, but far less than the latent track (a). The latent track with a steep entrance angle, higher than the "critical angle", will not be enlarged (b).

Different dielectrics have a different sensitivities to different particles and their energies. This means that some dielectrics will detect protons and others will not. Also, regarding the energies some dielectrics will practically always detect alpha particles, while other will have so called "registration threshold", which means that only those particles which in a certain part of their path through the dielectric, have linear rates of energy loss (dE/dx) higher than a threshold. These tracks will be registered in a given dielectric medium.

In principle the plastics have much lower registration thresholds than glasses or minerals and minerals. The polymers can detect light ions and the most commonly used polymer CR-39 or PADC (polyallyl diglycol carbonate) can detect even protons, while minerals can detect only the ions with Z>10 and also with higher energies. This can be used for a discrimination of different particles in the same environment. Differential annealing can be also used in this discrimination. The other two commonly used polymers: cellulose nitrate (LR-115) and polycarbonate (Makrofol), cannot detect

protons, and LR-115 has an upper energy threshold for alpha particles of 4-6 MeV, depending on the etching conditions. The sensitivity of CR-39 to protons implies a sensitivity to neutrons via (n,p) recoil reaction. For a purpose of a neutron dosimetry, the surface of an ATD is often covered by some (n, α) convertor – like matters which withholds ^{6}Li or ^{10}B.

Besides the standard chemical etching there is an electro-chemical etching (ECE) (Tommasino, 1973). The principle is to apply a strong electric field of ~50 kV/cm with high frequency of ~2 kHz during the chemical etching. The electric field rises around the tip of the cone of the etched track and an electrical break-through happens. The breakthrough is not complete due to the high frequency of the electric field. The break-through branch and it has a tree structure. The break-throughs are etched and new break-through occurs and the process continues. The electro-chemically etched tracks are much larger than the chemically etched ones.

Finally, the number of tracks per unit surface area, after subtracting background counts, is directly proportional to the integrated radon concentration in Bqh/m^3. A conversion factor obtained by controlled exposures allows conversion from track density to radon concentration. The whole process is schematically presented on Figure 4.

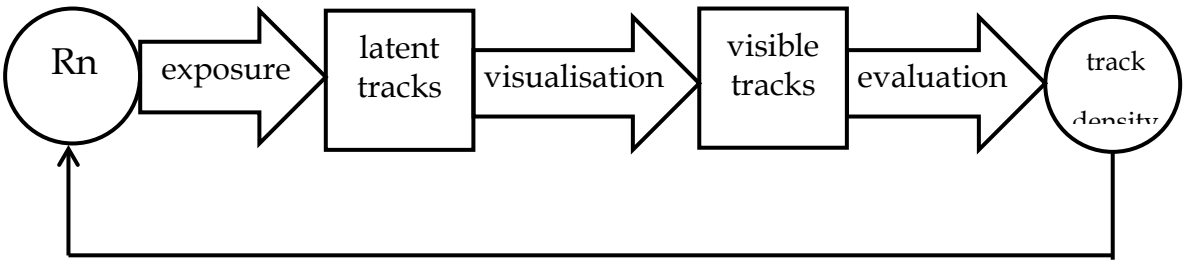

Figure 3.12: The scheme of the processing of an ATD regarding the radon measurements

3.1.1.2 Diffusion chamber for ATDs

A bare ATD exposed in indoor air will be sensitive both to radon and thoron. Normally, only radon should be measured, not the sum of radon and thoron. A sensitivity of ATDs to thoron can be avoided by placing the ATD in a diffusion chamber

with a large diffusion constant which will prevent thoron to enter inside the diffusion chamber, since the half-life of thoron (~55 seconds) is much shorter than the half-life of radon (~3.8 days).

The simplest diffusion chamber consists of a tube with a detector located at one end while the other end of the tube is open to the atmosphere ([18]). Effectively, the tube inside forms a diffusion zone which delays the arrival of thoron in the sensitive zone of the dosimeter, whereby the most of the thoron decay during the diffusion through the tube.

There are different permeation samplers which essentially present the above mention diffusion tube, whereby the open end is now covered by permeable membrane. The permeability of the membrane should be such that it completely prevents the thoron to enter the chamber, while the radon is unperturbed. This is not a hard task due to the big difference between the half-lives of these two isotopes. A membrane made of polyethylene or PVC, 10 μm thick is sufficient for this task. Moreover, the membrane improves stability by lowering the influence of humidity, electrostatic effects, temperature, dust, radon progenies etc. There is a solution where the diffusion chamber is sealed in plastic bag ([19]).

3.1.1.3 Radon/thoron discriminative detectors

There are several methods used for thoron measurement. One of them is the so called double alpha-track detector method (DTD) and both radon and thoron can be measured at the same time. Two different diffusion chambers are use, each one with its own alpha track detector. The radon and thoron have significantly different half-lives, (3.8 d) and (56 s) which makes them easy to be separated. One diffusion chamber should have large diffusion constant and it will detect only radon, because the thoron will decay before it reaches the ATD. The second diffusion chamber should have small diffusion constant and it will detect both radon and thoron. The ATD from the first diffusion chamber will measure the radon concentration, while the ATD from second will measure both the radon and thoron concentration. The thoron concentration is

obtained from a difference between these two ATDs. Obviously, the thoron lower detection limit will be lower and the measurement error will be higher value as it results from the difference between two readings. More information on DTD can be found in Tokonami et al. (2005a).

3.1.2 Activated charcoal adsorption detectors

Often this detector are simply called "charcoal canisters". These detectors are passive detectors. The Figure 3.5 shows the appearance of one charcoal canister and its scheme. The charcoal canisters are exposed to radon during 1-7 days. During that period the active sites capture the radon i.e. the radon is adsorbed by the charcoal. After the exposure the canister should be sealed and then transported for a measurement. In a relatively short time of several hours the equilibrium between the radon and its progenies is established. There are few methods to measure the radon in the charcoal. The most common method is to measure it directly on a gamma counter or spectrometer. In the second method, the alphas are counted using liquid scintillation vials containing few grams of activated carbon used in the measurement. The third method includes the usage of ATD exposed to the activated carbon. It was found that the sensitivity of ATDs in this case is almost 100 times higher than if a standard radon dosimeters with ATD were used.

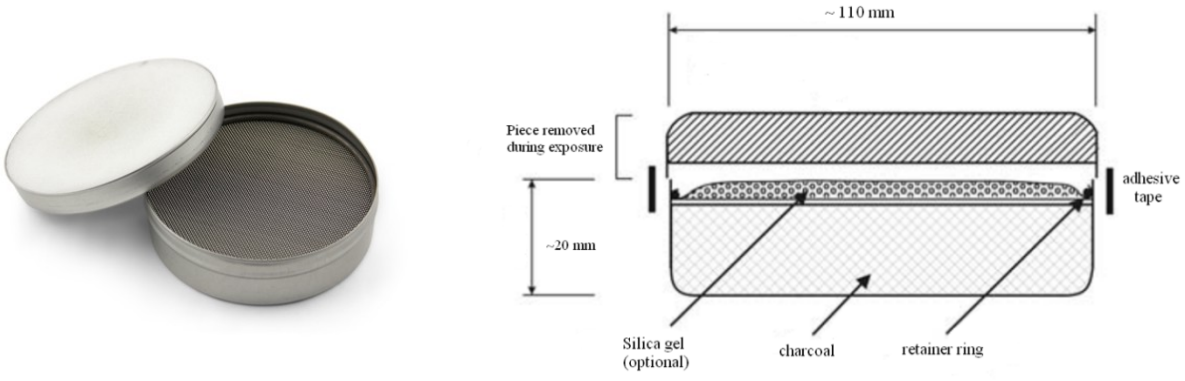

Figure 3.13: Charcoal canister. Usual appearance (left) and the scheme (right).

The canisters themselves may be open or used with a diffusion barrier to extend a measurement period or to prevent the thoron influence, especially if the method use a simple gamma counting. The response of the canisters is affected by humidity due to the competition in adsorption process, the canisters must be calibrated with different levels of humidity. Due to the process of adsorption and desorption they also must calibrated under different exposure times and temperatures. The charcoal canister method only provides a good estimation of the average radon concentration during the exposure time, only if the radon concentration variations are not significant. If a diffusion barrier is used on a charcoal canister it will lower the influence of the humidity, but also the influence of the air draft. Although the charcoal canister should be left after exposure for a short time of several hours to attain a equilibrium between radon and its progenies it should be measured in a time not much longer than the radon half-life (~3.8 days). Otherwise the measurement precision will suffer due to smaller activity.

3.1.3 Electrets ion chambers

Electret is an electric equivalent of a magnet. It has practically permanent electrical field due to the permanent dipole polarization. The most simple way to produce an electret is to heat a dielectric and to expose it to an electric field. Dipoles will be formed in the dielectric like they do in dielectrics in capacitors – Figure 3.6. Then after, the dielectric is cool down while it is still in the electric field and in some moment the dipoles will “freeze” keeping the permanent polarization. Development of high dielectric fluorocarbon polymers made electrets become reliable electronic components and their usage for practical purposes.

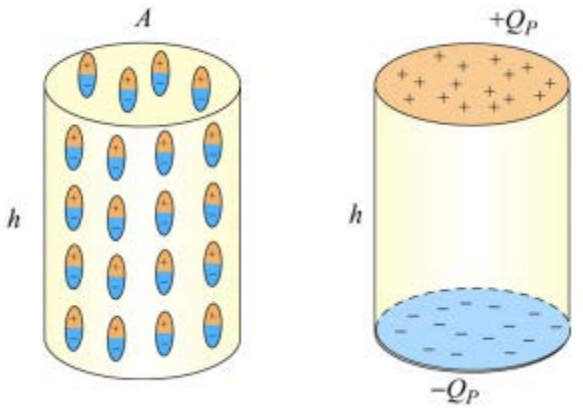

Figure 3.14: Scheme of a polarized dielectric. The electret is a permanently polarized dielectric.

Electret ion chambers are devices that function as passive and integrating detectors which measures effectively the average radon concentration during their exposure. In that sense they are analogue to the ATDs. As in the case of ATD diffusion chambers, only radon enters into the electret chamber by the diffusion process. The decaying radon and its progenies emit particles which ionize the air inside the chamber. The negative ions are collected by the positive electret side and the positive ions are collected by the negative electret side. This precipitation of opposite charge ions on the electret plates effectively discharge the electret and the amount of this discharge is proportional to the integral ionization during the exposure which is proportional to the exposure to radon. The average radon concentration of radon during the exposure is estimated the time duration of the exposure. The electret chambers may be designed for the short or long term exposures.

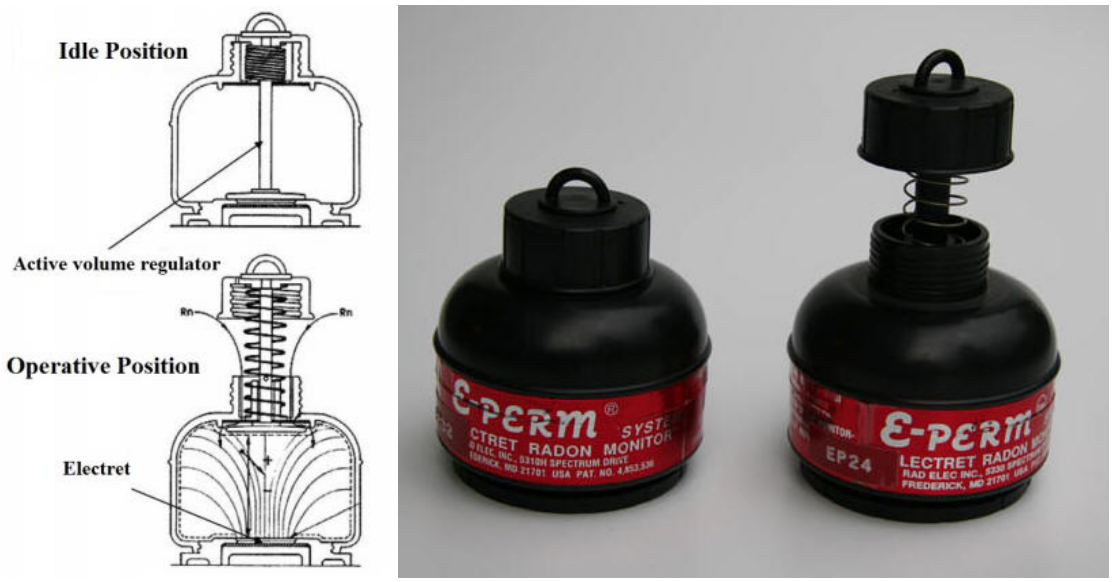

Figure 3.15: The electret ionization chamber. Scheme (left) and the appearance (right).

After the exposure the surface potential of the electret can be measured ([20]) and after this reading the electret surface potential can be reestablished and then used again in the radon measurement.

The advantage of electret dosimeter is that it can retain the information about the exposure to radon for a relatively long period of time. Also, it is quite rigid to the environmental influences. The disadvantage of the electrets is the response curve which is not reliable on very low and very high doses. The main disadvantage could be the fact that the electrets are also sensitive to the gamma radiation due to the fact that the gamma radiation also ionizes the air. This disadvantage could be solved by employment of another gamma sensitive detector.

3.1.4 Scintillation cells

Scintillation counting in the gaseous phase has been used form many years in the radon measurements. The oldest technique is proposed by ([21]), who was the first researcher who published about this technique. This type of scintillation counter is also known as Lucas cell. Since then many variations of this counter were manufactured.

The cell mainly consists of a glass vessel covered on inner side by a scintillating material, sometimes called phosphor – first known scintillating material. The microscopic light flashes induced by alpha particles emitted by radon and its progenies are hitting the phosphor are collected and amplified by a light amplifier. In the most of cases these light amplifier are photomultipliers. This technique could be used in field measurements, when air samples are collected inside scintillation cells. The grabbing of the air samples takes up to few minutes and then the samples could be taken to the laboratory for analysis. This method is called grab sampling. These types of measurements cannot capture the variation of the radon or radon decay product concentration. Grab sampling can be used in radon prospection, however it is not recommended for assessment of radon exposure and it is not reliable in the decisions about the mitigation of buildings.

Sensitivity depends of the scintillation cells depends on the volume and it could be slightly improved by increasing the volume of the flask, but it mainly depends on the duration of the counting. A sensitivity of a few Bq m^{-3} can be achieved and it can be further increased by electrostatical collection of ^{218}Po atoms directly on the detector ([22]). Also to improve characteristics of the measurement a coincidence of alpha and beta particles can be used. Sometimes the scintillation is used on filters for radon progenies, whereby the air is filtered through a filter with known flow and the filter is placed on the scintillator ([23]).

3.1.5 Active devices

To the contrary of previously described passive devices, the active devices allows to see the measured values of radon concentration immediately. Some devices also can measure thoron and radon and thoron progenies. The problem of active (electronic) devices is that they require the electric supply (a power grid or a batteries) and they have constrained autonomy. Therefore, they have a limited usage in the field work. The other disadvantage of the active devices is that are very expensive and fragile in

comparison to the passive devices. The advantage is that they can measure many parameters in the same time. The active part of the equipment could be ionization chamber or a semiconductor detector connected to a counter unit. The counting i.e. radon concentration is directly displayed on the instrument.

In contrast to passive devices most of the active devices are not based on the equipment in which the radon gas enters under natural drive - diffusion. Usually is pumped from the environment or extracted by means of a gas or liquid. The radon-charged air is forced to pass through a passageway around which the sorbent is placed. Sometime, the subsequent analysis of the adsorbent is carried out in the laboratory – like in case of use of scintilators for grab technique. The same scintilators can used with forced pumping (by means of forcing air through the detector), when the radon concentration is continuously measured.

There are numerous manufacturer and types of of these Instruments: alphameter manufactured by Alpha Nuclear Co. Canada, Alphaguard by Genitron Intruments. Germany, RMS-4501 manufactured by ECIL, lndia ([24]), the Radon gas meter TN-RN2000 manufactured by Thomson and Nielsen Electronics. Canada, the Atmos by Gamma Data, Sweden, the Rad7 manufactured by Niton, U SA; Prassi and Mod.4S models. by Silena Corp., Italy.

3.1.5.1 Continuous radon monitors

There are many commercially available active continuous radon monitors, which are using different detectors to measure radon: scintillation cells, ionization chambers or even a solid state silicon detector. The air could be measured or collected by pumping or by a plain diffusion. Continuous radon monitors (CRMs) need a power source and electric, computing circuitry in order to make more complex analysis. The result can be recorded in various time periods, integrated radon concentration could be calculated and so on. Each type of the CRM depending on its main detector can handle specific tasks. For example the solid state silicon detector can measure the alpha particle energy – perform alpha spectrometry, which also allows discrimination between different

alpha emitters: radon, thoron or their progenies ([25]) ([26]). Some devices need to dry the air in order to avoid the sensitivity on the influence of the humidity. In general, the lower detection limit of CRMs is around few Bq/m^3.

Figure 3.16: Examples of continuous radon monitors: RadStar Continuous Radon Monitor, RAD7, Sun Nuclear Model 1027

CRMs need routine calibrations to assure proper functioning and reliable results. On the Figure 8 few CRM devices are shown.

3.1.5.2 Specialized active devices

As it was mentioned, the active device based on the solid state silicon detector can perform alpha spectrometry and to differentiate different alpha particle emitters. This allows them to measure particular isotopes like radon progenies, thoron and thoron progenies.

Thoron continuous monitors

Continuous thoron monitors use electrostatic collection of charged radon decay products on a solid state silicon detector and detect emitted alpha particles. However, the indoor air is a mixture of radon and thoron and for example, thoron decay product ^{212}Bi emits the alpha particle of the same energy – 6 MeV as the radon progeny ^{218}Po which may influence both measurements, increase measurement uncertainty and finally it makes the process of the calibration very difficult. The thoron progeny ^{212}Po emits an alpha particle of highest energy among radon, thoron and their progenies – 8.8 MeV.

This can have an unwanted influence on radon measurements which use gross-alpha counting techniques. Obviously, CRMs used in a mixed radon-thoron atmosphere (which is very often a case), should be adjusted for this effect.

The indoor thoron concentration is not homogeneous as a consequence of short half-life of thoron. Therefore, the representativeness of thoron measurement is difficult to achieve. Obviously, the direct measurement of thoron progenies is very important. Opposite to radon, the thoron progenies have longer half-life than thoron itself - ^{212}Pb (10.6 h) as compared to thoron (~56 s). Consequently, the indoor thoron progenies concentration is less heterogeneous. In CRM/CTM it is also possible to apply radon/thoron discriminative measurements using the fact if the gas is moving only by the diffusion thoron will decay along its path, while radon will not.

Radon and thoron progenies measurement

Sometimes a more thorough assessment of the radiation exposure to radon or thoron is needed, especially at places where it is expect that the radon (or thoron) equilibrium factors will be significantly different. The direct measurement of the progenies can improve information about the equilibrium factor. All the progenies measurement are based on the collection of the progenies on filters and subsequent activity measurement of the filter. Examples of radon and thoron decay product measurement devices include gross alpha counters, integrating alpha-track decay product detectors, alpha-spectrometric devices with surface barrier detectors, and attached-unattached samplers ([27]).

3.2 Radon measurement in water

The radon presence in water is a consequence of its presence in the soil wherefrom the water originates. The radon from the soil is dissolved in the underground water. The water used by population in principle originate from the underground waters, whether it is the directly pumped underground water (for

example, artesian aquifer) or used from springs when the underground water reach the surface. In principle, negligible part of radon originates from the radium content in the water. The cancer risk for the population is in principle considered to be more significant due to the radon release from the water used in the house (washing, showering etc.), than due to the internal exposure than the risk from drinking water containing radon. The transfer coefficient which describes the amount of radon released from water, entering indoor air is ~10^{-4}. In general, the contribution to indoor radon concentration coming from the radon released from water is much smaller than the contribution from radon coming from ground sources where the house is built or the radon coming from the exhalation from the building materials. There are several methods and techniques for measurement of radon in water. The methods which are mostly used for measuring of radon in water are: liquid scintillation counting and the radon de-emanation.

3.2.1 Liquid scintillation

Liquid scintillation counting (LSC) is the most sensitive and widely used method to measure radon in water. The advantages of the liquid scintillation method are: simple sample preparation, low level of detection, high accuracy and precision and fast measurement. The radon is highly soluble in the organic solvants, and if the collected water sample is mixed with the organic solvent (toluene, xylene…) the radon dissolved in the water will be partitioned between the water/organic solvent mixture and the air in the vial where the sample is contained and will become available for measurement by LSC. The LSC method measures the activity of radon and decay products by the rate of photons emitted from the scintillation fluid. Disadvantage of the LSC technique is the initial cost of the counter and the need to perform the analyses in a laboratory i.e. the samples must be transported to the laboratory

3.2.2 De-emanation measurements

This is method is also widely used in the radon in water measurements. It is based on the de-emanation which extracts the radon from the water into a circulating radonfree gas which transports the radon to a radon measuring device. The water sample is placed in a bubbler which pushes the radonfree gas through the sample – bubbling it and extracting the radon from the water. The gas volume is five to ten times larger than the volume of the liquid. The extraction (de-emanation) of the radon from the water is achieved in normal temperatures. The transported gas is measured after ~3 hours when the equilibrium between the radon and its progenies is achieved. The low limit of detection is ~ 1 Bq/l.

3.3 Radon in soil measurements

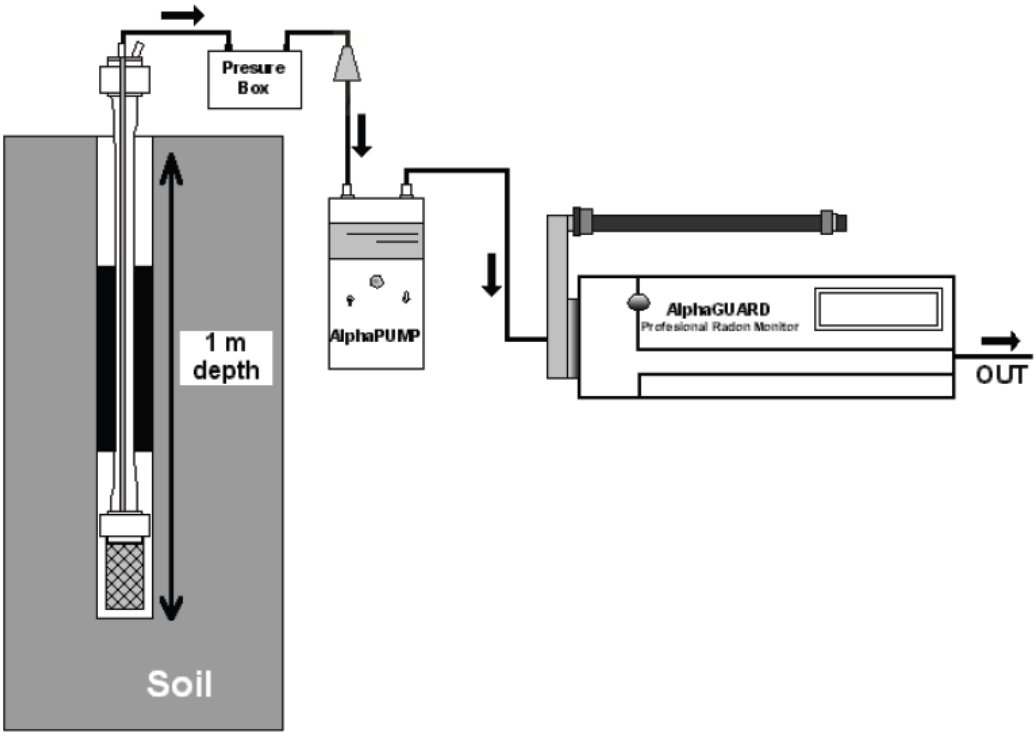

Figure 3.17: The schematic set-up of the AlphaGUARD detector and its accessories during the soil gas measurements [Kozak et al. 2004].

Radon detectors using solid-state detectors such as the AlphaGUARD radon monitor is shown on the Figure 3.9. It is based on use a chamber that allows for detection through alpha spectroscopy. In order to determine only the radon (^{222}Rn) concentration, the chamber needs to be closed tightly after filling it with soil gas for about 10 minutes, the time needed for thoron to decay [Koz04].

Another method for radon in soil measurement for geoscientific or geoengineering purposes is to bury the dosimeter in the soil at the depth of the hole of 60-70 cm. The measurement should be conducted carefully as the moisture can cause severe problems for in-ground measurements. The reproducibility of measurement of 13% can be achieved.

3.4 Long term and short term measurement

Radon measurements can be divided in two groups: short-term and long-term measurements ([28]). The short-term measurements can be used as a first indication about the radon concentration. The devices or methods used for this kind of measurements are charcoal canisters, electret chambers, grab technique, active devices. In short-term measurement the radon variation should be taken into account, with special attention to diurnal and seasonal variations. The radon concentration estimation in short-term measurement can significantly underestimate or overestimate average radon concentration. The short-term measurement directly depends on the activity of inhabitants. To assess the annual average radon concentration, the measurement must be conducted during the whole year. However, it is possible that even annual radon concentration can vary as year-to-year random variation in the same a home, depending on the weather. In addition, situations may arise where decay product measurements are necessary in order to improve the estimate of the overall radon dose to the individual.

Since high radon concentrations commonly occur during periods when homes are "closed up" (i.e. windows closed), a short-term measurement performed during this period, or season, can overestimate the yearly mean radon concentration. Alternatively, a short-term radon measurement performed during a period when the house has increased ventilation (e.g. windows open) can substantially underestimate the mean annual radon concentration. Therefore, in order to assess the annual average radon concentration within a home, devices that provide a long-term integrated radon measurement are preferred. However, it should be noted that even yearly radon concentrations in the same home can vary (Zhang et al., 2007). Sometime, it is necessary to measure radon progenies' concentrations in order to the estimate of the radon dose to the individual.

3.5 Calibration of radon measurement devices

Calibration of instruments for the radon measurement is very important as the wrong measurement will have a consequence of wrong risk estimation. There is a difference in the calibration of continuous radon monitors and the integrating measurement devices.

3.5.1 Calibration of continuous radon monitors

Continuous monitors are calibrated individually by the manufacturer or later by a reference laboratory, authorized and trained by the manufacturer. The calibration of continuous monitors have two important steps, besides the verification of the device functionality (batteries, charging, voltage, currents, wave patterns …): 1) the determination of the background by the exposure to the radon free gas and 2) verification of the calibration factor by exposure to a controlled reference atmosphere in a system for test atmospheres with radon.

After the calibration, a certificate of calibration of the reference laboratory is issued with the following information: 1) the condition of the device when it was received (damage, settings, voltage, background and calibration factor), 2) the measured background, 3) the measured response to the reference atmosphere – radon concentration (or calibration factor); 4) the new settings of the mentioned parameters, 5) the date the calibration.

3.5.2 Calibration of integrating and equilibrating devices

Integrating and equilibrating devices (alpha-track devices, electret ion chambers, charcoal devices), are not calibrated individually, but several detectors used in the field are exposed in a system for test atmospheres with radon, usually varying different parameters: radon concentration, exposure period, relative humidity and temperature. One responsible for the calibration insures that the device develops sets of calibration curves or algorithms, based on data from exposures in the system for test atmospheres with radon. The calibration curves produce values of the calibration factor for the calibrated device, in a function of the applied parameters (duration of exposure, electrical potential on electrets, ambient gamma background, relative humidity, temperature).

The calibration process must be repeated every time that the device is modified physically - the diffusion chamber is changed or different lot of charcoal, or every time that quality control data show or indicate the results are no longer reliable.

CHAPTER

4 Gamma spectrometry

Similarly to atoms that have energy levels characteristic for every element, the atomic nucleus has energy levels unique for each isotopes. When atoms de-excite, if it emits a photon with the highest energy in the range of several eV till a few hundreds of keV those are the X-rays. On the other hand, de-excitation of atomic nucleus is going through the emission of photons with an energy from several keV till several tens of MeV, known as gamma-rays. The well established method that allows measurement of gamma-rays and consequently identification and quantification of corresponding isotope is called gamma-ray spectrometry.

In this chapter a basic principles of gamma-ray spectrometry will be given: sources of gamma-ray radiation; the instrumentation necessary to detect gamma rays, then the principles of spectrum formation will be described as well as spectrum calibration in order to be able to unambiguously identify gamma decaying nuclei and be able to extract activity of the given samples.

4.1 Introduction

The gamma-spectrometry is widely used analytical method to identify and quantify gamma emitting nuclei in sample and has numerous advantages compared to radiochemical and mass spectrometry methods, since this method is non destructive, has an easy sample preparation, all gamma-ray emitting radionuclides present in medium can be identified in single analysis, it is possible to follow its full decay chain and finally has a low running cost.

Gamma-ray spectroscopy beside its usage in nuclear physics (nuclear structure, rare processes...) is widely used in:

- monitoring in nuclear facilities

- environmental physics
- health physics
- nuclear medicine
- science of materials
- bioscience
- forensic science
- archaeology...

Since X- and gamma-rays as photons do not have intrinsic charge, their passage through matter cannot be measured directly by its ionisation, but indirectly through their interaction with electrons in medium. There are three main interaction of photons with material that are important for gamma-ray spectroscopy: the photoelectric absorption, the Compton scattering and the pair production that were already described in introductory Chapter.

4.2 Sources of gamma-rays

The source of the gamma-rays can be defined as a macroscopic quantity of material that contains not only decaying atoms but carriers of the radioisotopes and material of the matrices as well. For the gamma- spectrometry, it is not only important activity and composition of the source, but its uniformity, self-absorption in the source, stability...

In general, there are two main types of emitters of gamma radiation:

- *Radioactive sources* that contain radioactive material deposited in the stable carrier from the same element of in the matrix of different elements of compounds. Some of typical examples are: a sample of 40K in the soil matrix, charcoal canister that consists of adsorbed Rn and its decay products, radiopharmaceuticals (like $^{99}Tc^{m}$ in water solution, ^{18}F in FDG)... Radioactive sources can be made without carrier or matrix and therefore

to consist only o radioactive material like: a layer of ^{241}Am deposited electrolitically; a ^{137}Cs source produced my mass separation...

- *Sources activated by external radiation* contains atoms of stable elements that are activated (became radioactive) by their irradiation with particles or photons (like samples activated by thermal neutrons i.e. (n,gamma) reaction, or (p, gamma) reaction).

According to dimension of the sources of radiation, their relative dimensions with respect to the size of the detector and source-detector distance, they can be classified into: point sources, surface sources and volume sources. Point source is a source which can be regarded as having negligible dimensions with respect to the detector. Similarly, for the surface sources thickness of the source can be neglected so it can be approximated as a disc with infinitesimal thickness. The sources whose dimensions cannot be neglected are volume sources.

In gamma spectrometry, almost all measurements are relative. The radioactive sample that is measured can be compared either directly using standard source that emits gamma-rays with the same energies or more often with a standard sources that emit photons at different energies. In ideal circumstances, measured source and calibration source have the same shape, density and chemical composition. This is usually not the case and there are different corrections (i.e. attenuation and intrinsic attenuation) that should be applied to compensate these difference. It is usually assumed that radionuclides inside the source are uniformly distributed which should be the case for liquid or gaseous sources or thin sources... Nevertheless, this is not always the case, for instance: for the samples irradiated in accelerators in which used beam has certain distribution with maximum in its center, the samples that are gradually changing phase from liquid to solid (like concrete) and therefore becoming subject of gravitational force... It is necessary to take all these imperfections into account to make proper correction on attenuation and absorption and to get reliable estimation

of activity of the sample. The gamma-rays emitted from the source should be then detected and quantified with some of the numerous gamma-ray detectors.

4.3 Gamma-ray detectors

The main principle of all radiation detectors it that through the interaction with detector material it is possible to ionise medium within the active volume of the detector. There are many different types of gamma-ray detectors and they can be classified by the type of active volume and the way electrical signal obtained for ionization of the active volume is collected. The choice of detector type to be used to detect gamma radiation depends on numerous factors: type of measurement (e.g. gamma dose rate measurements or gamma spectroscopy), activity of the source (e.g. activity of the highly irradiated samples or detection of the rare events), expected energy range of the source (X-ray spectrometry, environmental samples, or very high gamma-ray energies of cosmic rays), required uncertainty in determination of energy and/or activity of the measured source of gamma-ray radiation.

4.3.1 Gas-filled detectors

With the passage of gamma-rays through the gas, the molecules of gasses get ionised along the path by the means of interactions described in previous chapters. The created ion pair (a free electron and a positive ion) is guided with the applied electric field in the chamber and consequently the electrical signal is developed. Depending on the applied voltage in the detector, there are working regions of gas-filled detectors as indicated in Figure 4.1.

4.3.1.1 Ionisation chamber Proportional chamber

At low values of applied voltage, the drift velocity of created pairs of ions is small causing the recombination of the ions which as a consequence has a less collected

charge compared to the created ones. The first working region of gas-filled detector is ion saturation in which applied voltage is enough to prevent recombination, but small enough to prevent secondary ionisation. This in the working mode of ionisation chambers. One of the typical applications of the ionisation chambers is the measurements of gamma-ray exposure. Namely, exposure is defined as the amount of ionisation charge created in air and thus with a proper setting of ionisation chamber it is possible to measure the exposure. Ionisation chamber can be also used for the indirect measurement of absorbed gamma dose since absorbed dose for a given material is proportional to the number of produced ion pairs per unit mass formed in the gas.

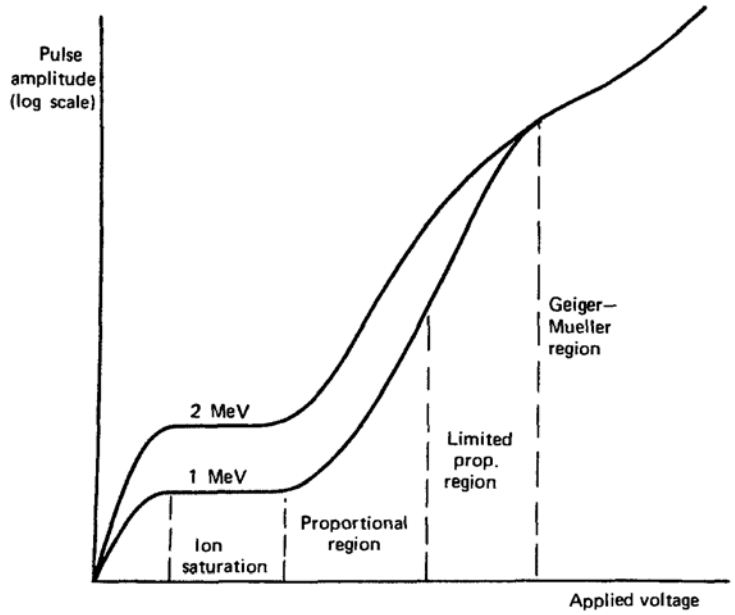

Figure 4.1. The working modes of ionisation gas-filled detectors as a function of applied voltage. The detector response is shown for two different energies deposited in the detector (Knoll).

4.3.1.2 Proportional chamber

With a further increase of applied voltage, created ion pairs will accelerate enough through the electric field so before recombination, they will have enough energy to cause secondary (or multiple) ionisation. In this region, known as proportional region, a gas multiplication is linear with the increase of applied voltage and collected charge is proportional to the primary number of ion. This mode of operation is characteristic for proportional counters. The proportional counters can be

used for the spectroscopy of X-rays and low energy gamma-rays. The spectroscopy of low-energy X-rays is based on the full absorption of the photoelectrons. The fraction of gamma-rays absorbed in the gas strongly decreases with the energy of incident photon energy. With the energy higher than several tens of keV, the counting efficiency becomes so small that proportional counter is not applicable anymore.

4.3.1.3 Geiger-Mueller Counters

With further increase of applied voltage, gas-filled detector first comes into region of limited proportionality, where some nonlinearities takes place. Namely, contrary to electrons that are quickly collected, drift velocity of positive ions is much smaller, so if they are generated in high concentration, they tend to alter the electric field in the detector and depending on the place of primary ionisation this response can be different causing the nonlinearities in the generated pulse as a function of applied voltage.

At sufficiently high voltage, the number of avalanches becomes dominant, the number of created positive ions increases significantly, quenching the electric filed and preventing additional multiplications. This region is known as Geiger-Mueller (G-M) region. It is characterised as the self-limiting process in which the secondary reactions will stop always with the same level of generated ions, not depending on the primary number of generated ion pairs. Therefore, the generated pulse is always the same, not depending on the type or energy of incident radiation.

In order to generate pulse from a G-M tube, it is necessary that only one secondary electron reaches a gas in a chamber. Therefore, efficiency to detect gamma-ray can be increased by increasing the thickness of the wall of G-M tube choosing a material with higher Z for the wall as well as for the gas. The efficiency of detecting gamma-ray in the wall is around several percent. With low gamma- and X-rays, probability for detection in the gas increases and can further be enhanced by choosing high-Z gasses such as Xe or Kr and counting efficiency can goes up to 100%.

The major disadvantage of the G-M counter beside the lack of energy information is a large dead time (the period after each event during which the detector is unable to detect another event). This makes G-M counter limited to the low counting rates.

4.3.2 Scintillation detectors

One of the oldest technique to detect ionizing radiation is using scintillation detectors. Scintillation detector consists of material (scintillator) that emits light when ionizing radiation interacts with the atoms of scintillator.

Some of the major properties that scintillation material should have are:

- material should convert ionizing radiation into detectable light with a high efficiency,
- the amount of created light should be proportional to the wide range of deposited energy,
- the material should be transparent to the created light and
- should have refraction index high enough to permit coupling to a photomultiplier tube,
- short decay time of induced luminescence in order to provide fast timing properties

In general, scintillation material can be divided in two categories: organic and inorganic. The choice of detector material depends on application for which the detector system is meant. The inorganic materials have better light yield and linear output, compared to organic ones. In addition, they can be constructed of material with a high Z-value and high density. These characteristics make them suitable for gamma-ray spectroscopy. On the other hand, organic scintillators are faster, the liquid and plastic ones can be made in very large volumes, so they are more suitable when a fast timing is required and when a large volume detectors of several meters are required.

The scintillation material is optically coupled to the photo-multiplication tube as presented in Figure 4.2. The light produced in scintillator hit the photocatode and via photoelectric effect is converted to electrons. Photoelectrons are then accelerated in the strong field of photomultiplier tube, creating a flash of electrons for hitting each electrode. Finally, electron shower of the order of 10^4 times more electrons compared to initially created ones reach the output anode. The magnitude of collected charge is proportional to the energy deposited in the scintillator.

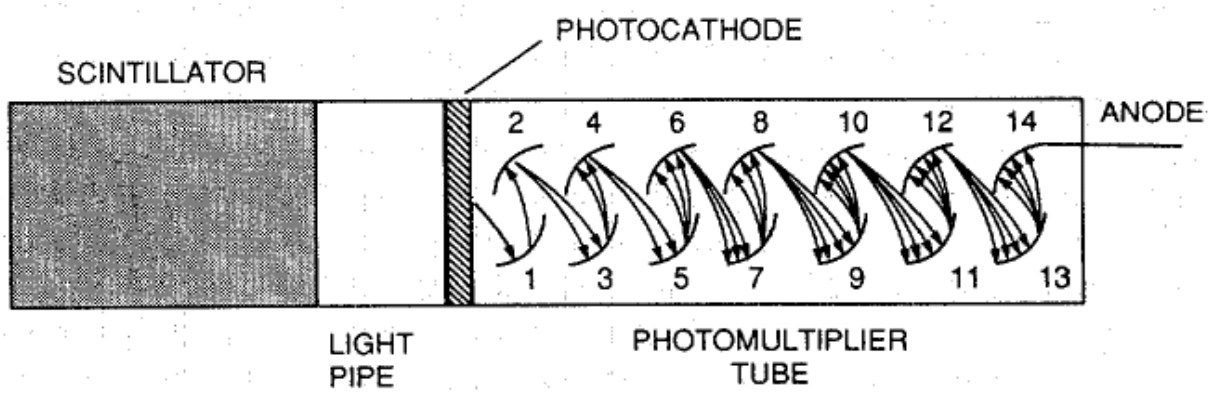

Figure 4.2. Schematic representation of scintillation detector: scintillator material, coupled to photomultiplier tube over light pipe. The electrodes in photomultiplier tube serve to allow successive electron cascade and the final charge is collected by exit electrode (anode)

Although, the output signal is proportional to the incident energy of the gamma-ray, final spectra is complex due to the numerous interactions of gamma-rays with material, statistical effects and so on. Detailed characteristics of detected spectra will be given in the following sections.

In Figure 4.3. is given comparison of two gamma-ray spectra obtained by two typical inorganic scintillation crystals: BGO (upper part) and NaI(Tl) (lower part) of the same size. A better energy resolution (ability of system to separate two adjacent peaks) is observed in spectra of sodium iodide (narrow peaks) on one side and higher efficiency of BGO (larger area under the photopeak) observed on the other side.

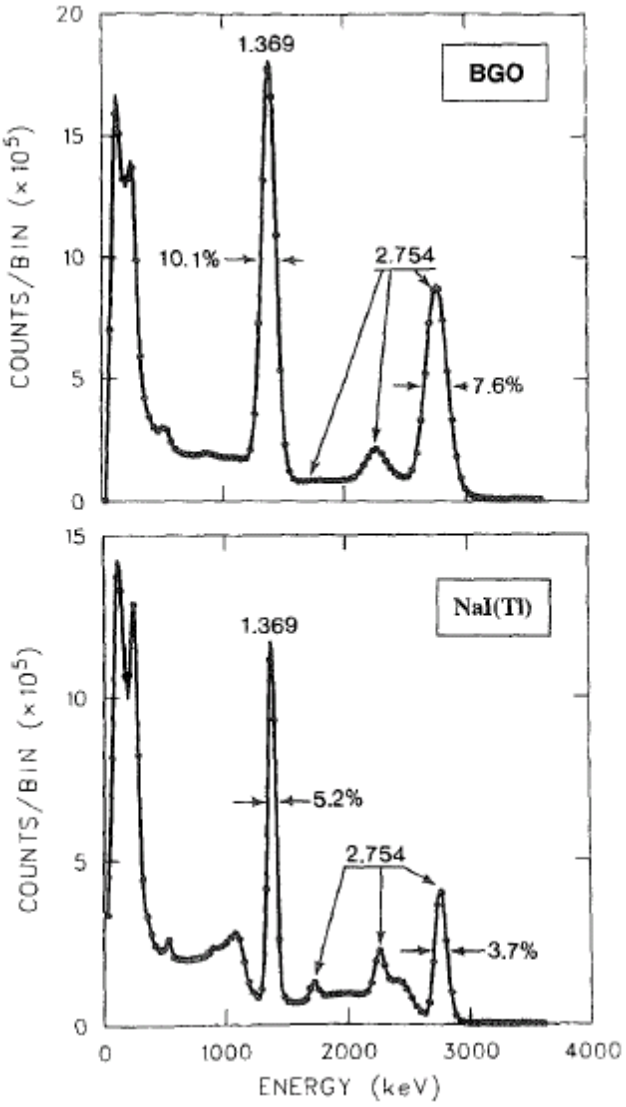

Figure 4.3. A gamma-ray spectrum obtained for two typical inorganic scintillation material: BGO (upper part) and NaI(Tl) (lower part) with the same crystal size. (taken from Knoll)

4.3.3 Semiconductors

Advantages of semiconductor detectors: densities of solids are 3 orders of magnitude higher that for gasses, making therefore possible to construct detectors of more compact dimensions.

In scintillation detectors, the major limitation is energy resolution since it is required many inefficient steps in order to generate output electrical signal: radiation

into light, light into photoelectrons, efficiency of collecting light, coupling of detector to the photomultiplier tube... Energy necessary to create one photoelectron is of the order of 100 eV and usually no more than a few thousands photoelectrons are created, limiting therefore resolution to the intrinsic statistical fluctuation.

The energy resolution can only be increased by generating more electrons (carriers of information) per incident radiation. The best energy resolution achieved up to date is using semiconductors in which the detector is a p-n junction. Information carriers are electron-hole pairs created by the passage of the radiation, in the depleted region that originates when a high inverse voltage is applied to p-n junction (the left hand side of Figure 4.4). Created electron-hole pairs are then drifted in opposite direction by a high electric field generating a signal. Since the ionization energy of both Ge and Si is around 3 eV, the number of carriers produced per incident radiation is at least 10 times higher than in the case of gas-filled and scintillation detectors providing therefore much better energy resolution which is confirmed in a comparison between energy resolution of spectra created by NaI and Ge detector (Figure 4.5)

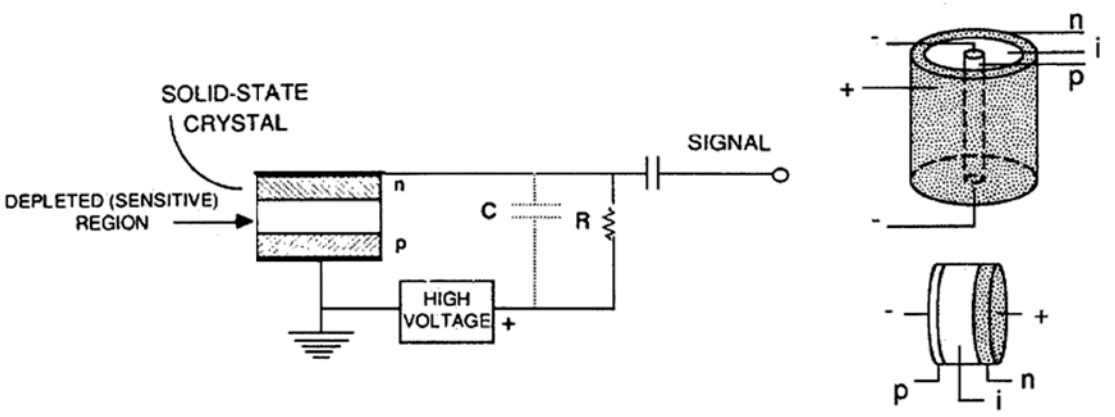

Figure 4.4. Schematic representation of semiconductor detector with reverse biasing (left-hand side); two typical HPGe detector configurations: coaxial and planar (top-right, bottom right side). Indicated are: p-type, n-type and i - depleted region

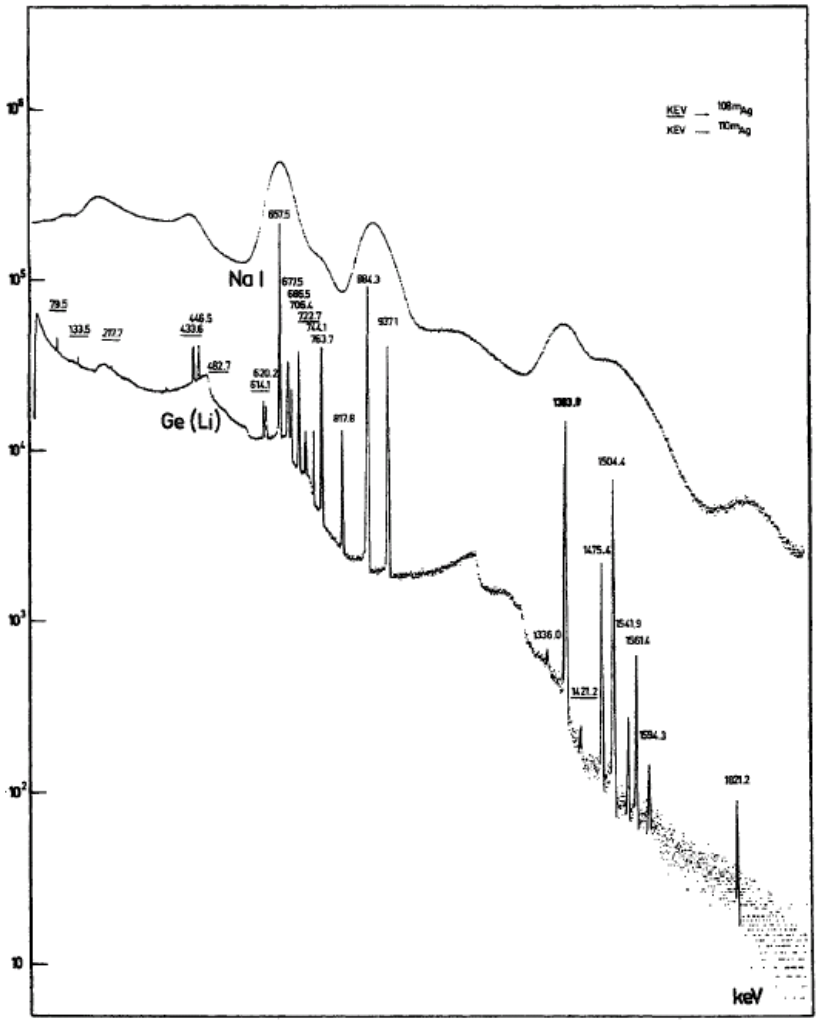

Figure 4.5. A comparison between energy resolution of ^{108}Ag and ^{110}Ag spectra created by NaI and Ge detector (Knoll)

The major characteristics: superior energy resolution, compact in size, relatively fast timing properties, effective thickness can varied depending on application for which is meant.

Among two dominant semiconductor materials Si is used for charged particle spectroscopy, while Ge is dominantly used for gamma-ray spectrometry, since germanium has much larger atomic weight compared to silicon and has a higher density favouring therefore interaction with gamma-rays. Another important advantage

of Ge with respect to the Si is the size of depleted region. The thickness of depleted region can be expressed as:

$$d = \left(\frac{2\varepsilon V}{eN} \right)^{1/2} \quad (20)$$

where e and ε are the electric charge and the dielectric constant respectively, V is the applied reverse voltage and N is concentration of impurities in the semiconductor.

In mid-seventies, it was developed technique to produce high-purity germanium detectors (HPGe) with impurities concentration reduced down to 10^{10} atoms/cm^3, while typical impurity concentration of Si detectors is of the order of 10^{13} atoms/cm^3.With usual Si detectors it is difficult to achieve depletion region thicker than 2-3 mm, while for HPGe detectors it can go to a few centimeters. In addition, the band gap (energy difference between valence and conductive band) for Si is 1.115 eV and for Ge is 0.665 eV, which means that electron can easier jump to valence zone in Ge, therefore being able to better discriminate small energy difference., which further leads to a better energy resolution. The valence electrons in materials with a small bandgap like in Ge, at room temperature can have thermal energy enough to jump into conductive band. Therefore, in order to provide that HPGe semiconductor can serve as a detector it is necessary to cool it down, usually to the temperature of liquid nitrogen.

Depending on a shape of crystal and how a detector is wired in a circuit, there are two main configuration: coaxial and planar configuration (top and bottom left hand-side of Figure 4.4). Coaxial configuration can be open-ended coaxial (as in Figure 4.4) or close ended. The crystals can be produced in the large sensitive volumes, thus having a large efficiency for gamma-rays. The radial electric field makes coaxial detector suitable for fast timing measurements. On the other hand, planar detectors have electric field perpendicular to the base of detector. They can be constructed with a small entrance window. In addition, the lower capacity of planar detectors provide them the best energy resolution, so they are favourable for detailed spectroscopy of low energy gamma- and X-ray.

4.4 Formation of gamma-ray spectrum

Although, the output signal is proportional to the incident energy of the gamma-ray, even for the monochromatic gamma-ray source, the obtained spectra is much more complicated than having just one gamma line. In this section, gamma-ray system necessary to build the gamma spectrum will be described as well as numerous features that are present in the gamma-ray spectrum.

4.4.1 Gamma-ray detection system with HPGe detector

As mention in the previous section, one of the best detectors for gamma-ray spectrometry is HPGe detector. The typical system for gamma-ray spectroscopy, presented in Figure 4.6. consists of: HPGe detector, high voltage power supply, preamplifier, amplifier, analogue to digital converter, multi-channel analyzer and a system for visualisation (computer).

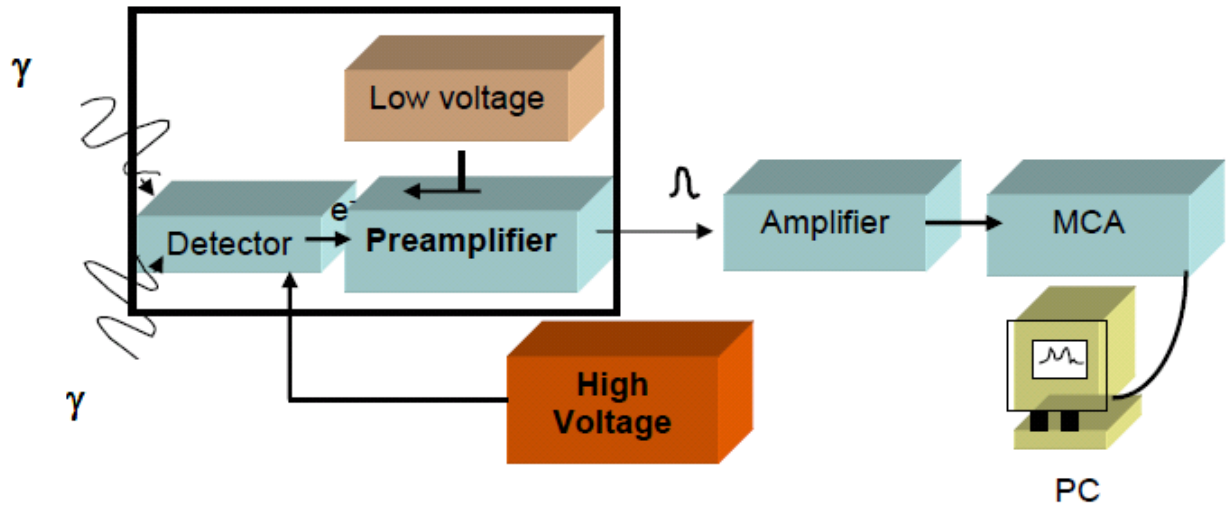

Figure 4.6. Typical gamma-ray spectrometry system

The whole process from detecting gamma-rays till their visual representation in a spectrum goes through several steps:

- gamma-rays interacts with matter in depleted region. The high voltage in the system is necessary to produce large depleted region
- created electron-hole pairs are drifted from the depleted region by high voltage applied
- These electrons/holes form a pulse that is increased by preamplifier. Preamplifier serves also to adopt high impedance of the detector to a low impedance of amplifier
- Created pulse is further increased and shaped with the amplifier
- These analog pulses are going to the analog-to-digital converter (ADC) which as a result give digital value (number) that is proportional to the generated pulse
- Each generated value from the ADC is stored in the multi-channel analyser (MCA) that gathers all information and present them in a real time
- Thus created spectra can be visualised and analysed using computer.

Newer generations of gamma-ray systems can use digital signal processing instead of analogue amplifiers allowing much faster respond.

4.4.2 Characteristics of gamma-ray spectrum

The pulse height spectrum of gamma-ray detectors in general depends on gamma-ray interaction with detector material. As already mention in Introduction chapter, there are three types of interactions relevant for gamma-ray spectroscopy: photoelectric absorption, dominant for gamma-ray energies up to several hundred keV; pair production dominant above 5 MeV of gamma-ray energy; and Compton scattering for energies between (see Figure 7 of Introduction).

Ideally, in the very large detectors, all interaction will take place in the detector. The scattered gamma-rays and annihilation photons will eventually undergo

photoelectric absorption and thus all energy of the gamma-ray will be deposited in detector and as a result, in the spectra will be present only full-energy peak.

In the case of real size detector, not all gamma-ray energy can be deposited in the crystal and consequently spectrum becomes more complicated. Schematic representation of gamma-ray interactions on real detector size as well as the influence of surrounding material on the detector response is given in Figure 4.7.

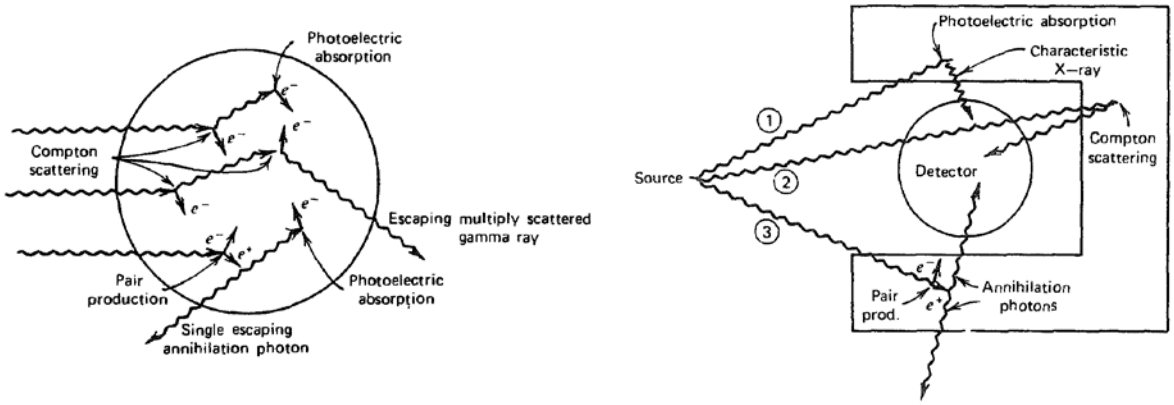

Figure 4.7. Interaction of gamma-rays with intermediate detector size (left-hand side) and influence of a surrounding material on a detector response. (Knoll)

Numerous interaction of gamma-rays with detector and surrounding material, gives a rise to a complicated gamma-ray spectrum even for a monoenergetic gamma-ray source. The gamma-ray spectrum of ^{137}Cs decaying by a single 662 keV photopeak energy is given in Figure 4.8. While in Figure 4.9. pulse height spectrum of ^{60}Co source decaying with two gamma-rays of 1173 keV and 1332 keV energy, respectively. In the figures are indicated characteristic features of gamma-ray spectra:

- **full energy photopeak:** represents a peak that arise when all energy of incident gamma-ray is deposited in the crystal by a single photoelectric interaction (or multiple followed by each Compton scattering)
- **Compton edge and Compton continuum**: In a Compton scattering two extreme interactions can takes place: in a grazing angle scattering the scattered angle of gamma-ray is close to 0°. From the kinematics, comes out that practically gamma-ray does not change the energy and no energy

is transferred to electron. In a head-on collisions, the incident gamma-ray is scattered by 180° and in this way, a maximum energy is transferred to an electron. This maximal energy deposited to electron is called **Compton edge** and for high gamma-ray energies, the Compton edge is shifted by 0.256 MeV from the full energy photopeak. Continuous part of the spectra between 0 keV and Compton edge is called **Compton continuum**.

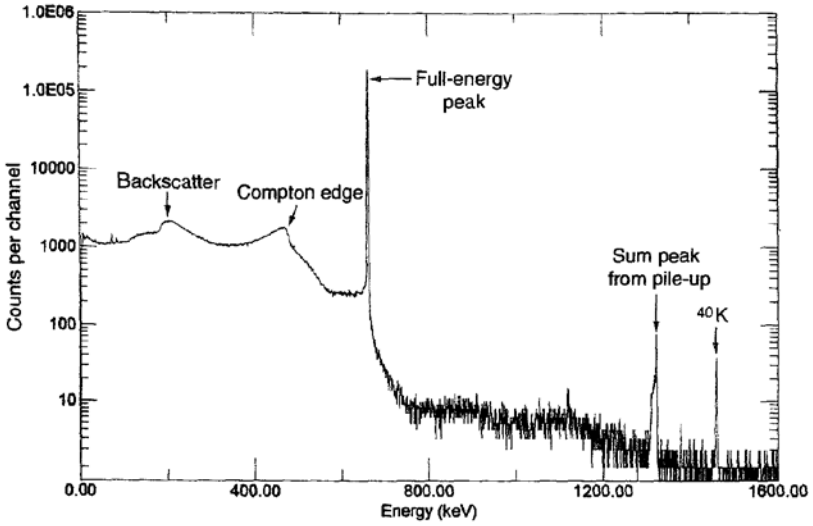

Figure 4.8. A pulse height spectrum of HPGe detector from ^{137}Cs source. Major spectrum features of spectrum: full energy peak, Compton edge, backscatter, sum peak, background peak are indicated

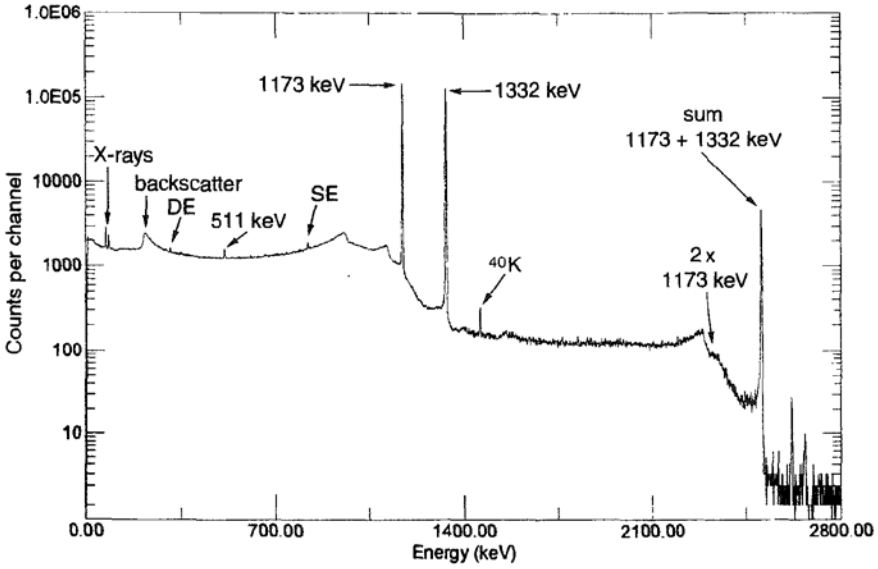

Figure 4.9. A gamma-ray spectrum of ^{60}Co source with its characteristic features

- **"Compton valley":** is the region between the Compton edge and full energy photopeak. It can origin from: multiple Compton scattering events, full photo absorption of gamma-ray that enters detector with a slightly reduced energy (e.g. due to small scattering in surrounding material), or from Compton scattered events from higher-energy peaks.
- **backscattered peak:** originates from the gamma-rays that have reached the detector after being scattered with an angles larger than 110°-120° in the material surrounding detector. The peak is the low-energy spectrum around 0.2-0.25 MeV.
- **single and double escape peak:** if incident gamma-ray energy is higher than 1022 keV, a pair production can take place and consequently a production of two 511 keV gamma-rays with positron annihilation. If one annihilation photon escapes the detector and the other is completely absorbed in detector, this will give a rise to peak that is located 511 keV from the full energy photopeak and is called **single escape peak**. If both annihilation peaks escape detector, the peak will be shifted by 1022 keV and is called **double escape peak**. Also, it is possible that one peak escapes, while the other is partially absorbed. This will raise a continuum in spectrum between two escape peaks.
- **annihilation peak:** When a pair production takes place in the surronding material and one of the annihilation photons is fully absorbed in the detector will give a rise to the 511 keV **annihilation peak.**
- **X-ray:** when photoelectric absorption takes place in surrounding material, near detector, it can generate characteristic X-rays (e.g. lead for instance from the shielding) that can be further detected by detector.
- **sum peak:** occurs for when nuclei is emitting two or more photons within the spectrometer resolving time. The sum peak can appear also for monoenergetic gamma-rays, but for sources with a high activity.

There are several other factors that additionally complicates spectra that are not directly indicated in Figures 4.8. and 4.9. These events are:

- **X-ray escape:** If the photoelectric absorption takes place near the surface of the detector, X-ray photon can escape from detector. This will give a raise to the peak which is by X-ray energy smaller than full-energy photopeak.
- **secondary electron escape:** by interaction of high energy gamma rays with material, high energy electrons can be produced which tend to leave detector material, leaving therefore a less energy to the system and therefore shifting a detector's response toward lower gamma-energies and reducing the intensity of full-energy photopeak.
- **bremsstrahlung escape:** The electron that scatters through detector material is emitting bremsstrahlung radiation. If this photons leave detector, they will produce the same effect as secondary electron escape.

4.4.3 Background radiation

Another important contribution to the spectrum that should be taken into account when analyzing it, is the background radiation. The major sources of the background radiations are primary and secondary components of cosmic radiation, primordial nuclides (nuclides that were created by nucleosynthesis in the same time with all matter of our solar system) and anthropogenic radionuclides that were created by man (e.g. atomic bombs, nuclear reactors). The primordial radionuclides, having the lifetimes comparable to the age of Earth (around $4.5 \cdot 10^9$ years) ^{232}Th, ^{235}U, ^{238}U (and members of radioactive decay series) and ^{40}K, are placed everywhere. Hence, they contribute to the internal background radioactivity: in material of detector and shield

that is placed around detector and external radioactivity: ancillary equipment, material of the building, air in the building (radon gas)...

Background radiation can significantly contribute to the spectrum, especially when low-activity samples are measured. Therefore, a lot of efforts is done to reduce the background radiation and depending on the application of the gamma spectrometry systems various techniques can be applied: *a passive shielding* - a use of 10-20 cm of lead shield around detector (for low background laboratories use very old lead, that do not have a radioactive component of ^{210}Pb, or do not have radioactive fallout from nuclear tests, nuclear accidents..., *an active shielding* - in which a various gamma-ray detectors (gas-filled or scintillators) are placed around the HPGe detector in order to reject events that have triggered the main and auxiliary detector at the same time. In this way, cosmic rays that reach detector or Compton scattered gamma-rays that exit detector can be rejected., *rooms with reduced gamma-ray flux*: a construction of rooms with clean material (sand, concrete) and covering walls with lead - to reduce gamma-rays from primordial radioisotopes, introduction of ventilation system to decrease Rn concentration in the room; *building underground laboratory:* reduces the cosmic-ray flux. Typical ceiling has a 0.5 mwe (meter water equivalent -) which stops around 10-20% of muons, while low background laboratory in Institute of Physics, Belgrade has a cover of 30 m.w.e. which reduces cosmic radiation about 10 times compared to laboratories at the surface.

4.4.4 Detector resolution and efficiency

Detector resolution was already described as an ability of detector to resolve two peaks close in energy and it is expressed at the Full Width at Half Maximum height of the full energy photopeak (FWHM). For the peaks that have Gaussian shape, FWHM can be expressed as:

$$FWHM = 2\sqrt{2\ln 2}\sigma \approx 2.355\sigma \qquad (21)$$

where σ is the standard deviation of Gaussian distribution of the peak.

Smaller the FWHM means a better energy resolution and separation of the peaks. And illustrative comparison between spectra created by BGO and NaI scintillators and NaI and HPGe detector is given in Figures 4.3 and 4.5 respectively. A statistical limits of resolution from different types of detectors are given in Table 4.1. As already explained in this chapter, the major factor influencing the resolution is the number of carriers produced in a detector for incident radiation, what is clearly seen from Table 4.1

Table 4.1 Statistical energy resolution for different types of gamma-ray detectors

Detector	Energy (keV) to produce e^-/ion pair	No. of e^- for 300 keV gamma ray	Energy resolution	High energy resolution
Ge	2.96	$1.0 \cdot 10^5$	0.86	1.6
Gas	30.0	$1.0 \cdot 10^4$	2.73	-
NaI	-	$1.0 \cdot 10^3$	22.6	30.0
BGO	-	$8.0 \cdot 10^2$	77.6	100.0

Another important parameter of detector is detector efficiency, It is the measure of sensitivity of detection system and in general it is the measure of number of pulses produced in the detector for a given number of gamma-rays. In gamma-spectrometry a several types of efficiencies are in use:

- **absolute efficiency:** ratio of the total number of detected and the total number of photons emitted by the source.
- **full energy (photopeak) efficiency:** the efficiency of producing full energy peaks over the all emitted gamma-rays from the source.
- **relative efficiency:** the ratio of the number of counts in the photopeak detected in HPGe detector and the number of counts in the photopeak of 3 in times 3 in. NaI scintillation detector.
- **intrinsic efficiency:** the ratio of the number of pulses produced by the detector and the number of incident photons. It does not depend on the

source-detector geometry and usually is used to compare different types of detectors.

Depending on the material of detector, its size and shape, the detection efficiency for different gamma-ray energies can be significantly different since different types of gamma-ray interaction with material are dominant at different energies. In order to estimate activity of the source it is necessary to know detector efficiency for a certain energy which is achieved by making efficiency calibration.

CHAPTER

5 Exhalation measurement and intercomparison

In this section the new method of the radon exhalation measurement is presented. Then after the method is compared with other standard methods and the results are compared. The advantages and disadvantages of the methods are also compared. The same cylindrically shaped sample of 7.1 cm diameter and 12 cm height was used as the reference sample for the measurement methods performed for in thesis. The sample was prepared by 'mixing' the travertine in Niška Banja, known for a high radium concentration, with the cement and sand. The accumulation chamber method is performed with the Solid State Nuclear Track Detector (SSNTD) and the active instrument partially simultaneously.

5.1 Theory background of the new gamma method of radon exhalation measurement

All the mentioned methods of radon exhalation measurement are measuring the exhaled radon directly. In herein described "gamma" method, the non-exhaled radon in the sample of building material is measured by gamma spectrometry, which then allows to estimate the exhaled radon.

A cylindrical sample with sealed lateral side and one base is considered (see Figure 5.1). The sample was left for a period of 10 half-lives of ^{222}Rn (~38 days) in order to achieve the equilibrium state. The homogeneity of the sample is assumed. The radon in the building materials exists in two phases: non-emanated (positioned in the mineral phase of the sample) and emanated (positioned in the air phase of the sample) – see Figure 5.1. The non-emanated part C_{ne} of the radon has a constant concentration in the sample:

$$C_{ne} = C_{Ra}(1-\varepsilon) \qquad (22)$$

where C_{Ra} is the ^{226}Ra concentration in the sample given in Bq kg^{-1}, ε is the emanation coefficient given in non-dimensional unit. C_{ne} is expressed in Bq kg^{-1}. The emanated

radon can diffuse through the air in the sample and its concentration C_e depends on the position on the axis of the sample.

$$D\frac{\partial^2 C_e(x)}{\partial x^2} - \lambda C_e(x) + \frac{C_{Ra}\rho\varepsilon}{p} = 0 \qquad (23)$$

where D is the radon diffusion coefficient in the given material, λ is the decay constant of the radon, ρ is the density of the material, p is a porosity of the material which defines the percentage of the air in a sample material. As the equilibrium is achieved the radon flux does not change with time, which means that its concentration at given position does not change with time, as well. It should be noticed that the concentration of emanated radon C_e is in principle expressed by Bq m^{-3} as it is in the air phase of the sample.

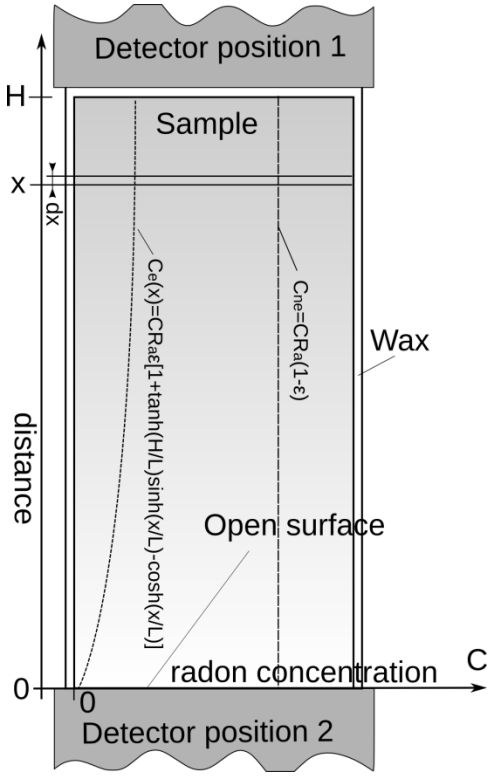

Figure 5.1: Scheme of the measurement setup showing the position of the sample and two possible positions of the detector. Radon concentrations (emanated and non-emanated), are also presented. The detector positions are shown as referent to the coordinate system referred to the sample. In reality the detector is at the same position, while the sample is turned upside down between measurements.

The general solution of the equation 36 is the following:

$$C_e(x) = A\sinh(x/L) + B\cosh(x/L) + C_{max} \quad (24)$$

where $L = \sqrt{D/\lambda}$ is the radon diffusion length in given material (m), $C_{max}=C_{Ra}\rho\varepsilon/p$ (Bq m^{-3}), D is the radon diffusion coefficient in the given material (m^2 s^{-1}), λ is the decay constant of the radon (s^{-1}), ρ is the density of the material (kg m^{-3}), p is a porosity of the material which defines the ratio of the air in a sample material.

Coefficients A and B are determined by boundary conditions:

$$C_e(x=0) = C_a(0) \rightarrow B = C_a(0) - C_{max}$$

$$\frac{\partial C_e(x=H)}{\partial x} = 0 \rightarrow A = (C_{max} - C_a(0))\tanh(H/L)$$

where H is the height of the sample. In the general case, C_{max} is much greater than $C_a(0)$ – the radon concentration in the air at point x=0, thus:

$$C_e(x) = C_{max}\tanh(H/L)\sinh(x/L) - C_{max}\cosh(x/L) + C_{max} \quad (25)$$

This equation is derived for the emanated radon inside the material (sample) expressed in Bq m^{-3}. In order to transform concentration in units of Bq kg^{-1} which is more convenient since this unit is used in the gamma spectrometry, both sides of equation are multiplied by factor p/ρ,which gives $C'_e(x)$ in Bq kg^{-1}:

$$C'_e(x) = C_{Ra}\varepsilon[\tanh(H/L)\sinh(x/L) - \cosh(x/L) + 1] \quad (26)$$

In principle, in gamma spectrometry and measurements of radionuclide concentrations in samples, the calibration is performed using radioactive standards of adequate geometry and matrix, whereby the homogeneous distribution of radionuclides within the standard is necessary. Radionuclide concentration C esitmated from the counting rate of gamma ray i - R_i of a given radionuclide in the sample is estimated by the following formula:

$$C_i = \frac{R_i}{mI_i C\eta^{(H)}}, \quad (27)$$

where, m – is the sample mass in kg, I_i – is the relative intensity of the gamma ray i of given radionuclide, $\eta^{(H)}$ is the calibration coefficient, where the superscript H is noting that the sample is in certain geometry i.e. a cylindrical shape with height $H$is presumed.

In the case of open sample where radon exhales at one side of the sample, the homogeneity is obviously not fulfilled ([29]). Thus, the counting rate estimation using a

chosen gamma ray i (i.e. chosen energy) of certain radon progeny is given by the following expression:

$$R_i = mI_i \int_0^H C_{tot}(x)\eta^{(H)}\eta_i(H-x)dx = \\ = mI_i C_{Ra}\eta^{(H)} \int_0^H [1+\varepsilon\tanh(H/L)\sinh(x/L) - \varepsilon\cosh(x/L)]\eta_i(H-x)dx \quad (28)$$

where $\eta_i(H\text{-}x)$ is a relative contribution to the counting rate of the layer of the sample of thickness dx at distance $(H\text{-}x)$ from a detector at the position 1 – see Figure 5.1.

The mentioned calibration coefficient $\eta_i(x)$ is needed in order to estimate the contribution of layer dx to the counting rate R_i. However, $\eta_i(x)$ cannot be determined experimentally and to make a calibration exclusively by Monte-Carlo is not recommendable. Thus, the solution is to determine an equivalent of $\eta_i(x)$ by a semi-empirical method, for instance by using the EFFTRAN package ([30]). The EFFTRAN package is used to transfer (recalculate) the calibration coefficient of a standard to a sample which has similar geometry (size and shape) and/or matrix (material). In order to calculate $\eta_i(x)$ as a relative contribution to the counting rate, instead original value of the calibration coefficient, a value 1 was used for the calculation (see Figure 5.2). Others simulation packages, like GEANT4 ([31]) could be also used.

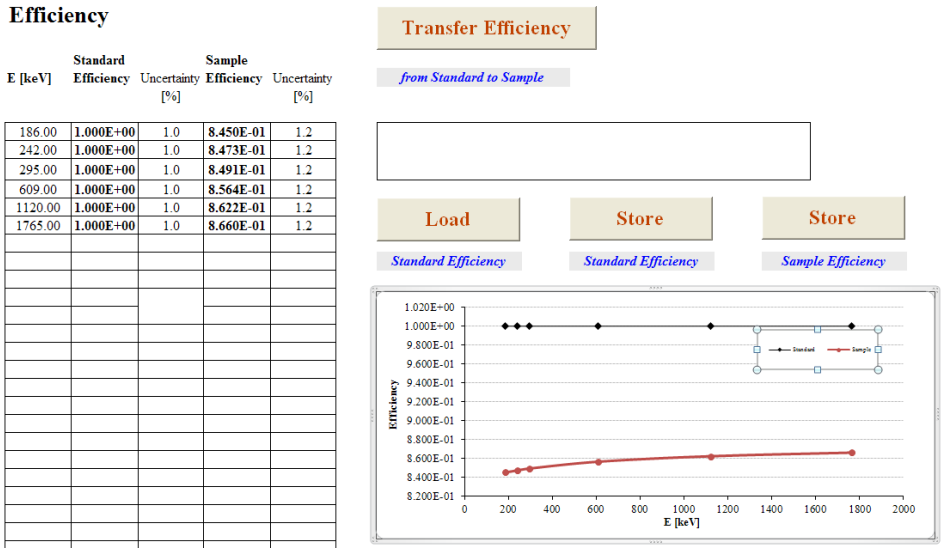

Figure 5.2: The EFFTRAN. Example of a calculation of the relative contribution factor $\eta_i(x)$ for one layer of thickness of 5 mm.

EFFTRAN application is limited to cylindrical detectors and samples and to axially

symmetrical setups. A separate version, called MEFFTRAN, exists for dealing with the Marinelli beakers. HPGe, NaI and LaBr3 detectors are supported. Gamma-gamma and gamma-X coincidences are taken into account and the correction factors for gamma rays are provided. EFFTRAN consists of three main separate Excel (.xls) modules: Efficiency Transfer, Coincidence Summing and Material (definition of new materials).

In this case, the EFFTRAN package was used to transfer calibration coefficient of a standard (35 mm radius, 35 mm high cylindrical box filled with sand) to layers of finite thickness Δx (instead of infinitesimal dx) at distance x from the detector (see Figure 1). The relative contributions to gamma ray i of layer dx (i.e. Δx, whereby in this case Δx = 5 mm) at the distances x = 0 mm, 5 mm, 10 mm up to (H – 5) mm are interpolated with polynomial function of tenth order - $\eta_{\Delta x}^{(i)}(x)$. The estimation of the function $\eta_{\Delta x}^{(i)}(x)$, for this case, is given in the Appendix I. As the function $\eta_{\Delta x}^{(i)}(x)$ is a relative contribution, the integral $\int_0^H \eta_{\Delta x}^{(i)}(x)$ must be normalised to 1:

$$A\int_0^H \eta_{\Delta x}^{(i)}(x)dx = 1 \;\Rightarrow\; A = \frac{1}{\int_0^H \eta_{\Delta x}^{(i)}(x)dx} \qquad (29)$$

Therefore, after the equation 41 is transformed accordingly, the final expression of radon concentration using a chosen radon progeny gamma ray i is:

$$R_i = mI_i C_{Ra}\eta^{(H)} \frac{\int_0^H \left[1+\varepsilon\tanh(H/L)\sinh(x/L)-\varepsilon\cosh(x/L)\right]\eta_{\Delta x}^{(i)}(H-x)dx}{\int_0^H \eta_{\Delta x}^{(i)}(x)dx} \qquad (30)$$

The unknown variables in the equation 43: the diffusion length – L and the emanation coefficient – ε. The ^{226}Ra concentration – C_{Ra} can be measured directly, while for the estimation of the L and ε, two independent measurements are needed. This could be obtained by a measurement of one sample with two detector positions (see Figure 1 and Figure 3). For the measurement at the detector position 2 (Figure 1) the orientation of x axes is changed and the function $\eta_{\Delta x}^{(i)}$ should be changed accordingly: $\eta_{\Delta x}^{(i)}(H-x) \rightarrow \eta_{\Delta x}^{(i)}(x)$. Thus the equation (9) for the detector position 2 is expressed as:

$$R_i = mI_i C_{Ra}\eta^{(H)} \frac{\int_0^H \left[1+\varepsilon\tanh(H/L)\sinh(x/L)-\varepsilon\cosh(x/L)\right]\eta_{\Delta x}^{(i)}(x)dx}{\int_0^H \eta_{\Delta x}^{(i)}(x)dx} \qquad (31)$$

The calibration coefficient $\eta^{(H)}$ is estimated directly using EFFTRAN by transfer of the calibration coefficient from the standard sample H = 3.5 cm to the measured sample of 12 cm.

After two measurements ([32]), ([33]) the system of two corresponding equations (43) and (44) with two unknown variables L and ε, has to be resolved numerically (for instance, the Mathematica package can be used).

The estimated concentration, of given radon progeny whose gamma ray i is used, is:

$$C_i = \frac{R_i}{mI_i\eta^{(H)}} \tag{45}$$

From equations 42 and 44:

$$\frac{C_i}{C_{Ra}} = \frac{\int_0^H \left[1+\varepsilon\tanh(H/L)\sinh(x/L)-\varepsilon\cosh(x/L)\right]\eta_{\Delta x}^{(i)}(H-x)dx}{\int_0^H \eta_{\Delta x}^{(i)}(x)dx} \tag{32}$$

and from 43 and 44:

$$\frac{C_i}{C_{Ra}} = \frac{\int_0^H \left[1+\varepsilon\tanh(H/L)\sinh(x/L)-\varepsilon\cosh(x/L)\right]\eta_{\Delta x}^{(i)}(x)dx}{\int_0^H \eta_{\Delta x}^{(i)}(x)dx} \tag{33}$$

This is the example how the set of equations 46 and 47, with the unknowns L and ε could be solved in Mathematica 10:

```
FindRoot[{Integrate[(1 + Eman*Tanh[118/L]*Sinh[x/L] - Eman*Cosh[x/L])* layers295[118 - x], {x,
0, 118}]/
    Integrate[layers295[118 - x], {x, 0, 118}] == 0.5816,
  Integrate[(1 + Eman*Tanh[118/L]*Sinh[x/L] - Eman*Cosh[x/L])*layers295[x], {x, 0, 118}]/
    Integrate[layers295[x], {x, 0, 118}] == 0.5703}, {Eman, 0.2}, {L,
  100}]
```

where *Eman* corresponds to ε and *layers295[x]* corresponds to $\eta_{\Delta x}^{295}(x)$. The Mathematica function *FindRoot* finds the solution of the given equations with unknown variables – in

this case *L* and *Eman (ε)*. The values 0.5816 and 0.5703 correspond to the ratio of C_i/C_{Ra}, measured in position 1 and 2 (see Figure 5.1).

It is important mention that C_{Ra} is estimated using the same ray *i* and same position, but with sealed sample. In that case the influence of uncertainty of the estimation of $\eta^{(H)}$ by EFFTRAN on the overall error is of the second order.

5.2 Intercomparison with other methods

5.2.1 Accumulation chamber with an active instrument method

Dimensions of the accumulation chamber are $0.263 \times 0.263 \times 0.424$ m^3 .

This method is widely used radon exhalation method and probably the most convenient one. When a sample is put in the sealed accumulation chamber, radon will exhale from the sample and it will accumulate in the chamber where it will eventually decay or escape if the chamber is not sufficiently tight. If the sample volume is not significantly smaller than the chamber volume (at least 10%), there is a significant probability that the radon atom, due to the diffusion, will return back into the sample. This is called the back diffusion. The exhalation measurements using accumulation chamber with an active instrument and the SSNTD (see Accumulation chamber with SSNTD method) were performed partially simultaneously. The measurements started at the same time and lasted 7 days, in the case of the measurement with the active instrument. This measurement was conducted using the RAD7 of Durridge Radon Instrumentation, calibrated in 2015, in National Institute for NBC Protection, Czech Republic. The radon concentration C(t) inside an accumulation chamber is described by the following expression :

$$C(t) = \frac{EA}{V\lambda_{eff}}\left(1 - e^{-\lambda_{eff} t}\right) + C_0 e^{-\lambda_{eff} t} \qquad (34)$$

where E is the radon exhalation rate of the sample, A is the surface area of the sample, V is the volume of the accumulation chamber; t is the time of exposure, C_0 is the initial radon concentration in the chamber and λ_{eff} is the effective radon removal probability defined as follows:

$$\lambda_{eff} = \lambda + \lambda_l + \lambda_b \quad (35)$$

where λ is the decay constant of ^{222}Rn, λ_l is the leakage probability and λ_b is the back diffusion probability. Since the sample volume is significantly smaller than the volume of the accumulation chamber the back diffusion can be neglected. C_0 is not considered since it was negligible. Diffusion of the radon from the outside air into the accumulation chamber is also neglected since the radon concentration in the outside air is two orders of magnitude smaller than the concentration inside the chamber. Sometimes the exhalation measurement is performed only using the linear part of the accumulating radon concentration when the exhalation rate can be approximated as follows:

$$E = \frac{bV}{A} \quad (36)$$

where b is the fitted slope of the first part of the concentration curve, up to 1800 min of measurement for which the linear approximation of the exponential function is applicable.

5.2.2 Accumulation chamber with SSNTD method

The exhalation rate of radon, measured by the accumulation chamber with the SSNTD is basically an integral measurement of the accumulation chamber, could be estimated by the following equation :

$$E = \frac{\rho_s V \lambda_{eff}}{kA} \frac{1}{t - \frac{1}{\lambda_{eff}}\left(1 - e^{-\lambda_{eff} t}\right)} \quad (37)$$

If the initial radon concentration C_0 is present exhalation is estimated as follows:

$$E = \frac{V\lambda_{eff}}{A} \frac{1}{t - \frac{1}{\lambda_{eff}}\left(1 - e^{-\lambda_{eff} t}\right)} \left[\frac{\rho_s}{k} - \frac{C_0}{\lambda_{eff}}\left(1 - e^{-\lambda_{eff} t}\right)\right] \quad (38)$$

where ρ_s is the track density on the SSNTD; k is the calibration coefficient for the detector. The factor ρ_s/k presents the exposure (sometimes referred as a dose) of the SSNTD. Since the C_0 cannot be determined in the SSNTD method, it is necessary to eliminate the radon in the moment when the accumulation chamber is sealed. The

measurement used for intercomparison was performed with the Landauer Radtrack2® SSNTD and it lasted for 37 days.

5.2.3 Charcoal canister method

Radon concentration measurements by charcoal canisters are often performed according to EPA 520/5- 87-005, David J. Grey, Sam T. Windham, 1987, EERF Standard Operating Procedures for Radon-222 Measurement Using Charcoal Canisters. The following gamma lines of radon progeny are used for the measurements: 295 KeV (^{214}Pb), 352 keV (^{214}Pb) and 609 keV (^{214}Bi). In the standard indoor radon measurement, the canister is exposed during 2–6 days and then measured on the gamma detector, where the quantity of the adsorbed radon is measured. The details of this method are given elsewhere ([34), ([35]). The radon concentration C_r is estimated using the following expression:

$$C_r = \frac{G - B}{tE_f C_f D_f} \quad (39)$$

where G is the total area of the three previously mentioned peaks, B is the total area of the background of the three mentioned peaks, t is the detector exposure time, E_f is the detector efficiency and C_f is the calibration factor of the radon adsorption rate on the charcoal. C_f strongly depends on the humidity. The correction factor of the radon decay during the exposure, D_f is approximated as follows:

$$D_f = e^{-\frac{0.693 t_s}{T_{1/2}}} \quad (40)$$

where t_s is the mid-time of between the start of the detector exposure and the start of the measurement and $T_{1/2}$ is the radon half-life. E_f is obtained from the efficiency calibration of spectrometry system. The product $C_r \cdot C_f$ is effectively a radon adsorption flux or in other words the flux of radon which is going to be adsorbed by the charcoal. The method of the radon exhalation measurement with charcoal canisters is based on the fact that the activated coal in the charcoal canister absorbs virtually all the radon atoms which enter into the canister. In that case the radon adsorption flux $C_r \cdot C_f$ is equal to the total exhalation rate E_t. Thus, there is not much sense to put a charcoal canister in the accumulation chamber. Instead, the charcoal canister can be attached directly to the surface of the sample whose radon exhalation rate is measured. It should be attached tightly in order to prevent radon to diffuse through the loose connection.

$$E_t = \frac{G - B}{tE_f D_f} \quad (41)$$

However, in order to obtain surface exhalation rate E, E_r has to be divided by the exhaling surface area A of the sample:

$$E = \frac{G - B}{tE_f D_f A} \quad (42)$$

5.3 Results

The comparison of all previously mentioned methods measurements is shown in (Table 5.1). and in (Figure 5.3) ([36]) ([37]) . The results are in agreement, however there is a certain discrepancy of the results, regarding the measurement uncertainties. This implies that there exists a variation of the exhalation rate and/or the uncertainty of the measurement is underestimated. Two parameters could influence the exhalation: the humidity and the atmospheric pressure variations.

Table 5.1: The results of the exhalation rate measurement of the same sample

	Exhalation [Bq s^{-1} m^{-2}]	Uncertainty [Bq s^{-1} m^{-2}]
Charcoal	0.028	0.004*
SSNTD	0.034	0.002
Active Long	0.0320	0.0003
Active Short	0.0293	0.0003
Gamma	0.0326	0.0014

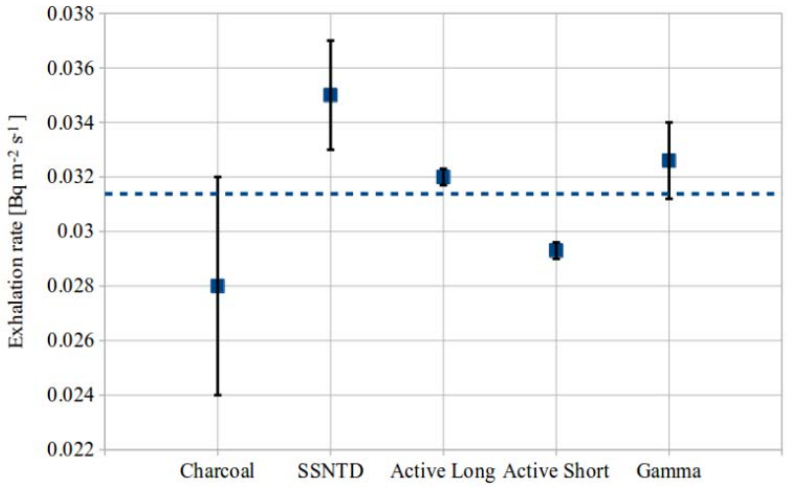

Figure 5.3: Graphical presentation of the results of the exhalation rate measurement of the same sample. The dashed line is a mean value of all measurements.

Measurement with active instruments in an accumulation chamber is in principle very simple. In comparison with the SSNTD method, the flaw of this method is that some of instruments do not the humidity control, like RAD7, since it constantly dry the air using a silica gel. However, this method offers possibility to estimate the influence of the leakage.

An advantage of the SSNTD method is the higher sensitivity i.e. lower Minimum Detectable Exhalation Rate (MDER), as this detector is measuring integral dose and consequently it can measure lower concentrations. Moreover, the diffusion chamber of the SSNTD design can significantly lower the MDER. In comparison to the measurement with the active instrument, the measurement with the SSNTD cannot be corrected regarding the accumulation chamber leakage, Therefore, the leakage have to be measured before (or after) the radon exhalation measurement itself. In this experiment, it was found that the leakage coefficient can vary for about 50%. The estimated exposure was 1540 ± 100 kBq h m^{-3} and the exhalation rate was E = 0.035 ± 0.002 Bq s^{-1} m^{-2} with the previously estimated λ_l = 2.4 10^{-7} s^{-1}. When the λ_l is significantly smaller than the radioactive decay constant of radon, its uncertainty and instability does not influence significantly the exhalation rate estimation. Nonetheless, in the SSNTD method, the leakage remains uncontrollable and its accidental change during the measurement cannot be detected. So, in principle, this method is reliable if the radon leakage coefficient is significantly smaller than the radon decay constant. In this intercomparison, the leakage coefficient is estimated during the simultaneous measurement by the SSNTD and the RAD7. The other disadvantage of the SSNTD is that its insensitivity to the initial background radon concentration in the accumulation

chamber. Both methods with the accumulation chamber, active and SSNTD method, require a longer measurement, although, the sample preparation is in principle very short.

The charcoal canisters used in this method have a relatively high minimum detectable activity of ~12 Bq m^{-3}, which corresponds to an exhalation rate of ~0.002 Bq s^{-1} m^{-2}, however this could be improved for at least one order of magnitude, by longer exposure period and longer gamma spectrometric measurement. It could be noticed that the measurement uncertainty is the highest for the charcoal method, however the duration of this measurement was far shorter than for the other methods, thus this uncertainty could be lowered by at least 5 times. This method has a potential to be used for in-situ measurements i.e. the charcoal canister may be attached directly to the inside wall of a building. Compared to the active method, it offers much more comfort to the inhabitants due as it is not noisy as an active instrument with an air pump.

The gamma method is a unique radon exhalation measurement method since it provides the measurement of the radon diffusion length and the emanation coefficient, which is a main advantage of this method. The estimated radon exhalation rate by the gamma method was 0.0326 ± 0.0014 Bq s^{-1} m^{-2}, while the radon diffusion length was 0.31 ± 0.03 m and the emanation coefficient 0.45 ± 0.02. The disadvantage of this method is a more complicated calculus and a longer sample preparation, since the equilibrium between the radon and its progeny must be attained.

Both the gamma and the charcoal methods do not need radon measurement equipment for the radon exhalation measurements and they are convenient for the laboratories which already have a gamma detector.

6 Conclusion

The gamma method is a unique radon exhalation measurement method since it provides the measurement of the radon diffusion length and the emanation coefficient. This presents a main advantage of this method. In this thesis, the feasibility of this method is proved and it is verified by the comparison with other methods.

Another advantage of the method is that it does not require a dedicated radon measurement equipment, whereas the radon exhalation measurement is performed only by use of a gamma detector (spectrometer) which is already used in the prospection of building materials regarding the radionuclides content. The energy saving policy have a consequence of increasing the average radon concentration in indoor air (even at higher floors) and the average population dose received from radon (Yarmoshenko et al., 2014), which will increase the importance of the measurement of radon exhalation from building materials. This method could be also used to test the mixture design of, for instance, concretes containing fly ash (Taylor-Lange et al., 2014).

The method is new and it could be expected that it could be improved. For example, it would be more convenient to make square sample as it is easier to cut and to prepare building material sample of that shape. Also, it would be interesting to examine the dynamic behaviour of this method. For example, to measure the concentration change immediately from the moment when one side of the completely sealed sample is open, to the moment when the steady state is achieved.

In Table 6.1 a tabular comparison of four exhalation measurement methods is given. The plus sign is marking an advantage. For example, the plus sign for the price means that it has a lower price.

Table 6.1: Tabular comparison of advantages and disadvantages of the exhalation measurement performed in this intercomparison.

	In-situ	MDER	Meas. Duration	Measures L, ε	Price	Precision	Chamber leakage	Moisture control	Background radon correction
Charcoal	+	-[a]	+	-	+[b]	-	NR	+	-
SSNTD	-	+	-	-	-	-	-	+	-
Active	+	+	+	-	-	+	+	-/+	+
Gamma	-	-	-[c]	+	+[b]	-	NR	+	+

NR – Not Relevant, L – radon diffusion length, ε – emanation coefficient, MDER – minimum detectable exhalation rate
[a] it is possible to improve it, principally for in-situ measurement
[b] under the assumption that a laboratory already has a gamma detector.
[c] the sample preparation included, otherwise the measurement is short

The choice of a method depends on different factors. For establishing a new method in a laboratory, it seems that the accumulation chamber with an active instrument is the most convenient. The charcoal canister method is simple, not expensive and offers a possibility of in-situ measurements. The SSNTD method seems to be the least advantageous; however it is a quite robust and reliable method. Gamma method is probably the most complicated method, however it is the only one which provides the emanation coefficient and the radon diffusion length which is also important regarding the protective attributes of a building material regarding radon.

Refferences:

[1]. *Evans, R. D.The Atomic Nucleus (1955).* the McGraw-Hill Book Company.

[2]. *ICRP 1987, International Commission on Radiological PLung cancer risk from indoor exposures to radon progeny.* Annals of the ICRP 50.

[3]. *ICRU 60 .1991. Fundamental quantities and units for ionizing radiation.*

[4]. (n.d.). NCRP 116. 1993.

[5]. *Von Hohenheim.T. 1925. Von der Bergsucht und anderen Bergkrankheiten.* (Vol. 1567). Springer Berlin Heidelberg.

[6]. *Fleisher 1988.*

[7]. *Fleischer et al 1965.*

[8] . *UNSCEAR . 2000. Sources and Effects of Ionizing Radiation.* New York: United

[9] . *Nazaroff W.W., Moed B.A., Sextro R.G. 1988. Soil as a source of indoor radon:*

[10]. Nazaroff W.W.. 1992. Radon transport from soil to air. *30*, 137-160.

[11]. Fleischer, R. L., Giard, W. R. 1980. Mogro-CampeDosimetry of environmental radon: methods and theory for low-dose. *Health physics , Fleischer, R. L., Giard, W. R., Mogro-Campero, A., Turner, L. G., Alter, H. W., & Gingrich, J. E. (1980). Dosimetry of envir39(6)*, 957-962.

[12] . Fleischer, R. L.. 1982. Alpha-recoil damage and solution effects in minerals: uranium isotopic disequilibrium and radon release. *uranium isotopic disequilibrium and radon release , 46(11)*, 2191-2201.

[13]. Sakoda A, Ishimori Y, Yamaoka K. 2011. comprehensive review of radon emanation measurements for mineral, rock, soil, mill tailing and fly ash. *rock, soil , 69*, 1422-1435.

[14]. Chen, C., Thomas, D. M.. 1995. Modeling of radon transport in unsaturated soil. *raJournal of Geophysical Research , 100*, 15517-15525.

[15]. Nazaroff W.W., and Sextro R.G. 1989. Technique for Measuring the Indoor 222Rn Potential of soi. *Environmental Science and Technology , 23*, 451-458.

[16] . Rogers, V.C.; Nielson. K.K.; Lehto, M.A.; Holt, R.B. September 1994. Radon generation and transport through concrete foundations. *EPA-600lR*, 94-175.

[17]. *Kulich et al 1988.*

[18]. Tommasino 1990. Radon monitoring by alpha-track detection. *Nucl , 17*, 43-48.

[19]. Tommasino L., Cherouati D.E., Seidel, J.L. and Monnin M.. 1986. plastic-bag sampler for passive radon monitoring. *Nucl , 12*, 681-684.

[20]. Kotrappa P., Dua K., Gupta P.G., Pimpale N.S and Khan A.N. 1984. Measurements of potential alpha energy concentration of radon and thoron daughters using an electret dosimeter. *Radiation Protection Dosimemtr , 5*, 49-51.

[21]. *Lucas H.F. . 1957. Improved low level alpha-scintillation counter for radon.* (Vol. 28 (9)). Rev. Sci. Instr.

[22]. (n.d.). Bochiccio F.and Risica S . 1990. Active radon and radon daughter monitors. In Proc. Int. Workshop on Radon. Monitoring in Radioprotection. *Environmental Radioactivity and Earth Science* , 110-121.

[23]. *Bovi M., Baldassini P. and Porcu I. 1993. Radon monitoring diffusion device.* Italian Patent.

[24]. *Singh B. 1992. Earthquake prediction studies in Kangra valley and Punjab. Thesis.* Amritsar (India): Guru Nanak Dev University.

[25]. Tokonami S et al.1996. Calculation procedure of potential alpha energy concentration with continuous air sampling. *Health Phys , 71*, 937-943.

[26]. Iimoto T et al. 1998. Continuous 220Rn concentration monitor using an electrostatic collection method. *Radiat Prot Dosimetry , 77*, 185-190.

[27]. Cheng YS et al. 1992. Use of a graded diffusion battery in measuring the activity size distribution of thoron progeny. *J. Aerosol Sci , 23*, 361-372.

[28]. Quindós LS, Fernández PL, Soto YL. 1991. Short versus long-term indoor radonmeasurements. *Health Physics , 61*, 539-542.

[29]. Awhida, A., P. Ujić, I. Vukanac, M. Đurašević, A. Kandić, I. Čeliković, B. Lončar, and P. Kolarž. 2016. Novel method of measurement of radon exhalation from building materials. *Journal of environmental radioactivity , 164*, 337-343.

[30]. Vidmar T. 2005. EFFTRAN - a Monte Carlo efficiency transfer code for gamma-ray spectrometry. *Nuclear Instruments and Methods , A 500*, 603-608.

[31]. *GEANT4. 2003. https://geant4.web.cern.ch/geant4/.*

[32]. A. Awhida, P.ujic, I. Celikovic . 2017. New gamma method for the radon exhalation measurement from building material. *IcETRAN* (pp. 1-3). Kladovo.Serbia: Proceeding of 4th international conference on electrical.

[33]. P.Ujic, I.Celikovic, A.Awhida, B.Loncar .septembar 2017. Merenje ekshalacije radona iz gradevinskih materijala Zbornik radova xxIx simpozijum Drustva za zastitu od zracenja Srbije., (pp. 219-224).

[34]. Pantelić, G., Eremić-Savković, M., Živanović, M., Nikolić, J., Rajačić, M. and Todorović, D. 2014. uncertainty evaluation in radon concentration measurement using charcoal canister. *Appl. Radiat. Isot , 87*, 452–455.

[35] . (n.d.). Živanović, M. Z., Pantelić, G. K., Krneta Nikolić, J. D., Rajačić, M. M. and Todorović, D. J. 2016. Radon measurements with charcoal canisters: temperature and humidity considerations. *Nucl. Technol. Radia* , 65-72.

[36]. (n.d.). Awhida, A., Ujić, P., Pantelić, G., Kolarž, P., Čeliković, I., Živanović, M., ... & Lončar, B.2016. AD-HOC INTERCOMPARISON OF FOUR DIFFERENT RADON EXHALATION MEASUREMENT METHODS. *Radiation Protection Dosimetry* , 1-5.

[37]. A. Awhida1, P. Ujić2, P. Kolarž3, I. Čeliković2, M. Milinčić4, A. Lončar4, B. Lončar. 2017. MERITS AND DEMERITS OF DIFFERENT METHODS FOR RADON EXHALATION MEASUREMENTS FOR BUILDING MATERIALS. *RAD Conference Proceedings*, *2*, pp. 132-136.

Образац 5.

Изјава о ауторству

Име и презиме аутора: AHMED ALI SALEM AWHIDA

Број индекса: 4048/2014

Изјављујем

да је докторска дисертација под насловом

Novel method for measurement of radon exhalation from building materials

Нови метод за мерење ексхалације радона из грађевинских материјала

- резултат сопственог истраживачког рада;
- да дисертација у целини ни у деловима није била предложена за стицање друге дипломе према студијским програмима других високошколских установа;
- да су резултати коректно наведени и
- да нисам кршио/ла ауторска права и користио/ла интелектуалну својину других лица.

Потпис аутора

У Београду, 16.10.2017.

_____

Образац 6.

Изјава о истоветности штампане и електронске верзије докторског рада

Име и презиме аутора : AHMED ALI SALEM AWHIDA

Број индекса : 4048/2014

Студијски програм : Инжењерство материјала

Наслов рада : Novel method for measurement of radon exhalation from building materials

Нови метод за мерење ексхалације радона из грађевинских материјала

Ментор : БорисЛончар

Изјављујем да је штампана верзија мог докторског рада истоветна електронској верзији коју сам предао/ла ради похрањена у **Дигиталном репозиторијуму Универзитета у Београду.**

Дозвољавам да се објаве моји лични подаци везани за добијање академског назива доктора наука, као што су име и презиме, година и место рођења и датум одбране рада.

Ови лични подаци могу се објавити на мрежним страницама дигиталне библиотеке, у електронском каталогу и у публикацијама Универзитета у Београду.

Потпис аутора

У Београду, 16.10.2017

_____

Образац 7.

Изјава о коришћењу

Овлашћујем Универзитетску библиотеку „Светозар Марковић“ да у Дигитални репозиторијум Универзитета у Београду унесе моју докторску дисертацију под насловом:

Novel method of measurement of radon exhalation from building materials

Нови метод за мерење ексхалације радона из грађевинских материјала

која је моје ауторско дело.

Дисертацију са свим прилозима предао/ла сам у електронском формату погодном за трајно архивирање.

Моју докторску дисертацију похрањену у Дигиталном репозиторијуму Универзитета у Београду и доступну у отвореном приступу могу да користе сви који поштују одредбе садржане у одабраном типу лиценце Креативне заједнице (Creative Commons) за коју сам се одлучио/ла.

1. Ауторство (CC BY)

2. Ауторство – некомерцијално (CC BY-NC)

3. Ауторство – некомерцијално – без прерада (CC BY-NC-ND)

4. Ауторство – некомерцијално – делити под истим условима (CC BY-NC-SA)

5. Ауторство – без прерада (CC BY-ND)

6. Ауторство – делити под истим условима (CC BY-SA)

(Молимо да заокружите само једну од шест понуђених лиценци.
Кратак опис лиценци је саставни део ове изјаве).

Потпис аутора

У Београду : 16.10.2017.

_____

1. **Ауторство**. Дозвољавате умножавање, дистрибуцију и јавно саопштавање дела, и прераде, ако се наведе име аутора на начин одређен од стране аутора или даваоца лиценце, чак и у комерцијалне сврхе. Ово је најслободнија од свих лиценци.

2. **Ауторство – некомерцијално**. Дозвољавате умножавање, дистрибуцију и јавно саопштавање дела, и прераде, ако се наведе име аутора на начин одређен од стране аутора или даваоца лиценце. Ова лиценца не дозвољава комерцијалну употребу дела.

3. **Ауторство – некомерцијално – без прерада**. Дозвољавате умножавање, дистрибуцију и јавно саопштавање дела, без промена, преобликовања или употребе дела у свом делу, ако се наведе име аутора на начин одређен од стране аутора или даваоца лиценце. Ова лиценца не дозвољава комерцијалну употребу дела. У односу на све остале лиценце, овом лиценцом се ограничава највећи обим права коришћења дела.

4. **Ауторство – некомерцијално – делити под истим условима**. Дозвољавате умножавање, дистрибуцију и јавно саопштавање дела, и прераде, ако се наведе име аутора на начин одређен од стране аутора или даваоца лиценце и ако се прерада дистрибуира под истом или сличном лиценцом. Ова лиценца не дозвољава комерцијалну употребу дела и прерада.

5. **Ауторство – без прерада**. Дозвољавате умножавање, дистрибуцију и јавно саопштавање дела, без промена, преобликовања или употребе дела у свом делу, ако се наведе име аутора на начин одређен од стране аутора или даваоца лиценце. Ова лиценца дозвољава комерцијалну употребу дела.

6. **Ауторство – делити под истим условима**. Дозвољавате умножавање, дистрибуцију и јавно саопштавање дела, и прераде, ако се наведе име аутора на начин одређен од стране аутора или даваоца лиценце и ако се прерада дистрибуира под истом или сличном лиценцом. Ова лиценца дозвољава комерцијалну употребу дела и прерада. Слична је софтверским лиценцама, односно лиценцама отвореног кода.